

AD-A198 946

4

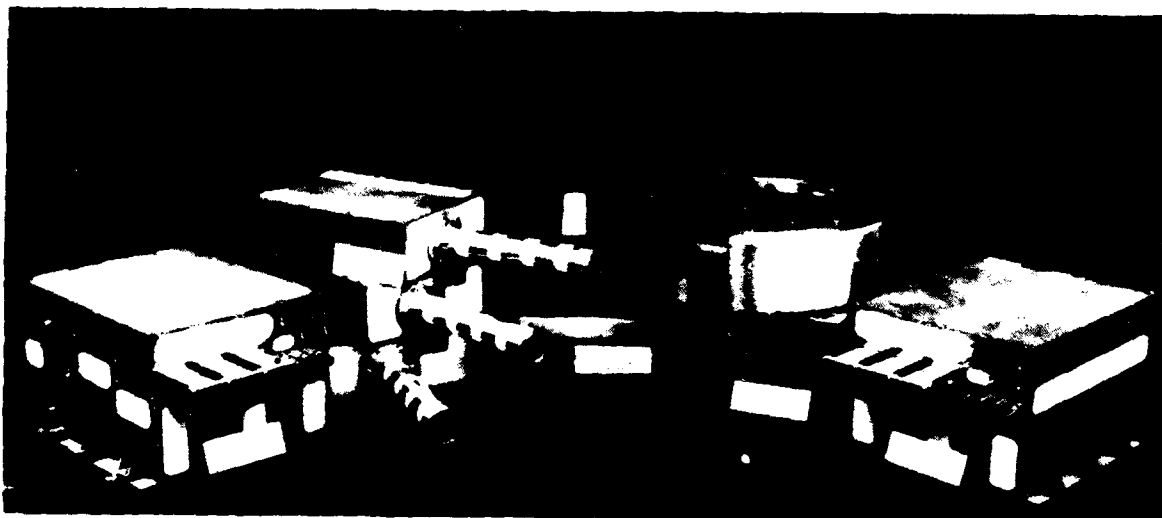
# Energetic Particles and Ion Composition Experiment for CRRES

Interim Technical Report

Prepared for The Office of Naval Research  
Space Physics Program  
Under Contract N00014-83-C-0476

June 30, 1988

DTIC  
ELECTE  
SEP 02 1988  
S H D



DISTRIBUTION STATEMENT A

Approved for public release;  
Distribution unlimited.

 **Lockheed**

Research & Development Division  
LOCKHEED MISSILES & SPACE COMPANY, INC.  
Palo Alto, California 94304

Unclassified

SECURITY CLASSIFICATION OF THIS PAGE

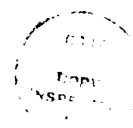
REPORT DOCUMENTATION PAGE

Form Approved  
OMB No 0704-0188

|   |  |   |   |
|---|--|---|---|
| 1a REPORT SECURITY CLASSIFICATION:<br>Unclassified  |  | 1b RESTRICTIVE MARKINGS   |   |
| 2a SECURITY CLASSIFICATION AUTHORITY  |  | 3 DISTRIBUTION / AVAILABILITY OF REPORT<br>Unlimited, cleared for public release and sale.              |   |
| 2b DECLASSIFICATION / DOWNGRADING SCHEDULE  |  | 4 PERFORMING ORGANIZATION REPORT NUMBER(S)  |   |
| 4 PERFORMING ORGANIZATION REPORT NUMBER(S)  |  | 5 MONITORING ORGANIZATION REPORT NUMBER(S)  |   |
| 6a. NAME OF PERFORMING ORGANIZATION<br>Lockheed Missiles and Space Company  | 6b OFFICE SYMBOL<br>(if applicable)                | 7a. NAME OF MONITORING ORGANIZATION<br>Office of Naval Research   |   |
| 6c. ADDRESS (City, State, and ZIP Code)<br>Department 91-20, Building 255<br>3251 Hanover Street<br>Palo Alto, CA 94304   |  | 7b ADDRESS (City, State, and ZIP Code)<br>Code 1114SP<br>800 North Quincy Street<br>Arlington, VA 22217 |   |
| 8a. NAME OF FUNDING / SPONSORING ORGANIZATION<br>Office of Naval Research   | 8b OFFICE SYMBOL<br>(if applicable)<br>Code 1114SP | 9 PROCUREMENT INSTRUMENT IDENTIFICATION NUMBER<br>Contract No.<br>N00014-83-C-0476                      |   |
| 8c ADDRESS (City, State, and ZIP Code)<br>800 North Quincy Street<br>Arlington, VA 22217  |  | 10 SOURCE OF FUNDING NUMBERS  |   |
|   |  | PROGRAM ELEMENT NO<br>61153N  | PROJECT NO<br>4149  |
|   |  | TASK NO<br>4149   | WORK UNIT ACCESSION NO<br>4149169   |
| 11 TITLE (Include Security Classification)<br>Energetic Particles and Ion Composition Experiment for CRRES<br>(unclass)   |  |   |   |
| 12. PERSONAL AUTHOR(S)<br>J. M. Quinn and R. R. Vondrak   |  |   |   |
| 13a. TYPE OF REPORT<br>Interim Technical  | 13b TIME COVERED<br>FROM 8/83 TO 6/88              | 14. DATE OF REPORT (Year, Month, Day)<br>88 / 06 / 30   | 15. PAGE COUNT  |
| 16 SUPPLEMENTARY NOTATION   |  |   |   |
| 17. COSATI CODES  |  | 18. SUBJECT TERMS (Continue on reverse if necessary and identify by block number)                       |   |
| FIELD   | GROUP  | SUB-GROUP   | Magnetospheric Modeling; CRRES Satellite; Energetic Particles; Ion Mass Spectrometers; Trapped Radiation; Space Radiation Effects |
| 20  | 08   |   |   |
| 20  | 09   |   |   |
| 19. ABSTRACT (Continue on reverse if necessary and identify by block number)<br>The ONR-307 Energetic Particles and Ion Composition instrument payload will measure the energetic particle and plasma environment of the Earth's radiation belts and inner plasma sheet. The payload has been successfully designed, built, and tested for flight on the Combined Release and Radiation Effects Satellite. The instruments were integrated with the spacecraft and tested with the integrated system. This mission, originally scheduled for shuttle launch in July, 1987, will now be launched on an Atlas Centaur in June, 1990. The ONR-307 payload is currently undergoing final adjustments and calibration activities prior to re-integration with the spacecraft in May, 1989. Procedures have been developed and documented for on-orbit operation of the payload and acquisition of the data on digital tapes. |  |   |   |
| 20 DISTRIBUTION / AVAILABILITY OF ABSTRACT<br><input type="checkbox"/> UNCLASSIFIED/UNLIMITED <input checked="" type="checkbox"/> SAME AS RPT <input type="checkbox"/> DTIC USERS   |  | 21 ABSTRACT SECURITY CLASSIFICATION<br>Unclassified   |   |
| 22a NAME OF RESPONSIBLE INDIVIDUAL<br>R. Gracen Joiner  | 22b TELEPHONE (Include Area Code)<br>202-696-4203  | 22c OFFICE SYMBOL<br>1114SP   |   |

TABLE OF CONTENTS

| TITLE   | PAGE |
|---|------|
| Abstract -----  | 1    |
| Background -----  | 2    |
| Progress to Date -----  | 6    |
| Summary and Future Activities -----                             | 11   |
| References -----  | 12   |
| Appendix A - ONR-307-3 Instrument Description -----             | A-1  |
| Appendix B - ONR-307-8-1,2 Instrument Description -----         | B-1  |
| Appendix C - ONR-307-8-3 Instrument Description -----           | C-1  |
| Appendix D - Statement of Conformance for ONR-307 Payload ----- | D-1  |
| Appendix E - ONR-307-3 Detector Calibration Report -----        | E-1  |



|                  |                                     |
|------------------|-------------------------------------|
| Approved For     | <input checked="" type="checkbox"/> |
| By               |                                     |
| Date             |                                     |
| Initials         |                                     |
| Signature        |                                     |
| Handwritten: A-1 |                                     |

ABSTRACT

The ONR-307 Energetic Particles and Ion Composition instrument payload will measure the energetic particle and plasma environment of the Earth's radiation belts and inner plasma sheet. The payload has been successfully designed, built, and tested for flight on the Combined Release and Radiation Effects Satellite. The instruments were integrated with the spacecraft and tested with the integrated system. This mission, originally scheduled for shuttle launch in July, 1987, will now be launched on an Atlas Centaur in June, 1990. The ONR-307 payload is currently undergoing final adjustments and calibration activities prior to re-integration with the spacecraft in May, 1989. Procedures have been developed and documented for on-orbit operation of the payload and acquisition of the data on digital tapes.

## BACKGROUND

The Combined Release and Radiation Effects Satellite (CRRES) is a joint NASA/DOD program which was originally planned to be carried out in two phases following a shuttle launch. The NASA phase of the mission, planned for execution in Low Earth Orbit (LEO), consists of several chemical releases in combination with onboard diagnostic instrumentation, measurements from other satellites, and ground based observation. Following the NASA phase of the mission, the spacecraft was to be boosted to Geosynchronous Transfer Orbit (GTO) to initiate the DOD phase. Following the Challenger accident the CRRES mission was restructured in order to allow the earliest possible launch. CRRES is now scheduled to be launched directly into GTO on an Atlas Centaur in June, 1990. The number of NASA chemical releases have been reduced, and the releases will now be performed in GTO during operations of the DOD instruments.

The ONR-307 payload, the Energetic Particles and Ion Composition (EPIC) experiment, consists of four instruments to be operated continuously during the CRRES mission in support of Navy objectives. Specifically, these objectives are to obtain the necessary plasma composition and energetic particle data over an extended period of time and with sufficient pitch angle resolution throughout the earth's radiation belts such that accurate environmental models, suitable for engineering purposes, can be constructed. The EPIC experiment will measure two critical components of the environment:

- 1) Energetic magnetospheric plasma, including composition, in the energy range 0.1 to > 1000 keV. This component of the space environment is the principal cause of spacecraft surface charging, degradation of sensitive spacecraft surfaces, and ionospheric disturbances that disrupt critical communications paths. In addition, some portion of this magnetospheric plasma is ultimately transported into the inner magnetosphere and energized to become part of the radiation belts.

- 2) Energetic electrons in the energy range 20 to 5000 keV and protons in the range 0.5 to 100 MeV. These energetic trapped components of the radiation belts penetrate deeply into spacecraft systems where they cause degradation of microelectronic components, charging/discharging of internal dielectrics, such

as coaxial cables, CMOS devices etc., and ultimately limit mission lifetime. These electrons, when precipitated out of the radiation belts into the atmosphere/ionosphere, enhance ionization of the D and E region ionosphere and can disrupt communications paths from ELF to HF.

In order to assure complete measurements of these key components, the EPIC payload uses four instruments of three different designs. The ONR-307-3 Spectrometer for Electrons and Protons measures energetic electrons and protons using a design derived from the highly successful SC-3 instrument developed for the Office of Naval Research for flight on SCATHA. The ONR-307-8-1,2 Low Energy Ion Mass Spectrometers measure ion composition at low to medium energies. These spectrometers are also based on instruments developed for the Office of Naval Research, first for the pioneering S3-3 mission, and later for SCATHA. The ONR-307-8-3 Medium Energy Mass Spectrometer uses an entirely new design, developed to extend the range of ion composition measurements well above those covered by the ONR-307-8-1,2 type of instrument. Descriptions of each of the instruments will be presented in the next section and in appendices to this report.

The measurements of the EPIC instruments, when combined with data from complementary instruments from other laboratories, will provide comprehensive, synergistic data to address Navy and DoD objectives. The extensive data base to be obtained in both space and time will provide the basis of greatly improved modeling of the inner and outer radiation belts, suitable for engineering design and analysis purposes in future DoD missions.

One of the critical results of the CRRES mission will be a determination of the effects of the radiation environment on a broad range of microelectronic components. Specifically, CRRES will directly correlate the measurement of radiation effects on microelectronics with simultaneous in situ radiation measurements. These correlations will be performed in parallel with the development of improved radiation belt models. Accurate models of the space radiation environment, together with an understanding of its effects on spacecraft systems, are of primary importance to the design, optimization, and operation of DoD space systems.

One of the most important life-limiting elements of DoD reconnaissance, communication and manned platforms in space is the radiation environment. Current program requirements demand operational spacecraft lifetimes of 5 to 10 years in near-earth orbit. Such long operational lifetimes demand that considerable attention be given to shielding and radiation-hardened electronic parts. Military space systems must also be designed to survive the even more extreme radiation effects from nuclear weapon bursts in space.

Radiation shielding creates significant weight and cost impacts on many DoD missions. Uncertainties in the amount of shielding required leads to conservative design practices which adversely impact available payload weight capability. Our present understanding of the earth's radiation belts, based on two decades of measurements, has been synthesized by the National Space Data Center into models of the electron and proton populations that provide the principal threat to satellites. For several reasons the accuracy of these models in defining the environment that a particular satellite mission will encounter is only good to a factor of 3, i.e. a 300 percent uncertainty. Of the many factors responsible for this large uncertainty, the dynamics of the radiation belts with solar activity, the limited region of space and temporal duration covered by the measurements, and the variability in the capabilities and accuracy of the measuring instrumentation are paramount. To significantly improve on the current radiation belt models, therefore, all of these limitations must be improved upon. The unique orbit of the CRRES mission, the comprehensive set of measurements and the long mission duration provide great promise for substantial improvements in future radiation belt modeling.

Because of the variety of orbits used by the DoD and the complexity of the radiations encountered it is essential that a comprehensive radiation measuring payload include:

- 1) Discrimination of the various particle types and masses, i.e. electrons, protons, and heavy ions.
- 2) Measurement of the energy spectra of the various particle species since this directly translates into the penetrating power through shielding.

- 3) Complete pitch angle coverage with good angular resolution since this provides the ability to map particles down the field lines from the point of observation. Measurements of the complete pitch angle distribution at the geomagnetic equator from  $0^{\circ}$  (along the field line) to  $90^{\circ}$  (perpendicular to the field line) with good angular resolution completely defines the entire particle population on that field line at all altitudes.
- 4) The ability to sample all of the magnetic field lines as close to the geomagnetic equator as possible since this will define the environment of the entire radiation belts.
- 5) Nearly continuous temporal coverage over a period of several years to provide statistically meaningful fluxes over the highly dynamic variations experienced as a result of solar and geomagnetic storms and substorms.

The CRRES orbit and the comprehensive measurements to be made by the ONR 307 instrumentation will enable us to satisfy all of the above requirements to a high degree.

Under the Office of Naval Research contract, N00014-83-C-0476, the Lockheed Space Sciences Laboratory has designed, developed and tested the EPIC instruments, integrated them with the CRRES, and supported system level testing of the integrated spacecraft. Due to delays in the launch of CRRES, all instruments have been removed from the spacecraft and returned to Lockheed. The EPIC instruments are currently undergoing minor modifications, testing, and calibration activities prior to their re-integration with the spacecraft, currently expected to occur in May 1989.

## PROGRESS TO DATE

Progress to date under contract N00014-83-C-0476 has included the design, development, and test of the ONR-307, EPIC payload. The instruments have been integrated with CRRES and have completed system level testing activities. Following these tests, the instruments were removed and returned to Lockheed during the spacecraft storage period.

The EPIC payload consists of four instruments of three different types. The Spectrometer for Electrons and Protons (SEP), designated ONR-307-3, measures electrons in the energy range 20 - 5000 keV and protons in the range 0.5 - 100 MeV. The energy ranges are covered with fine, programmable energy resolution. Very good pitch angle resolution is provided by 3 degree FWHM collimation. In order to obtain nearly complete pitch angle coverage over the CRRES orbit, the instrument uses three identical particle telescopes, mounted at carefully optimized angles to the spacecraft spin axis. Each telescope uses a stack of surface-barrier silicon detectors with active anticoincidence shielding. Various logic combinations of the detector elements determine the particle types and energy ranges that are measured. The SEP instrument is based on the highly successful SC-3 instrument developed for ONR and flown on SCATHA. The SC-3 instrument continues to operate after more than 9 years on orbit. Figure 1 shows the SEP instrument, consisting of the sensor package with three particle telescopes, the analyzer package, and the interconnect cable. A more detailed description of this instrument, its capabilities, and measurement goals is given in Reference 1 and included as Appendix A.

The Low Energy Ion Mass Spectrometers (IMS-LO), designated ONR-307-8-1 and ONR-307-8-2, are two identical instruments which measure ion composition in the energy range  $E/q = 0.1 - 32$  keV/e. The two instruments are mounted at different angles to the spacecraft spin axis in order to optimize pitch angle sampling. The IMS-LO instruments use crossed electric and magnetic field Wien filters, followed by 180 degree electrostatic analyzers and channeltron sensors to determine ion energy/charge and mass/charge. Three parallel analyzers are used within each instrument to cover different segments of the full energy range. The instruments may be commanded to sweep through the full mass range, to alternately lock on any four selected masses, or to alternate between the two

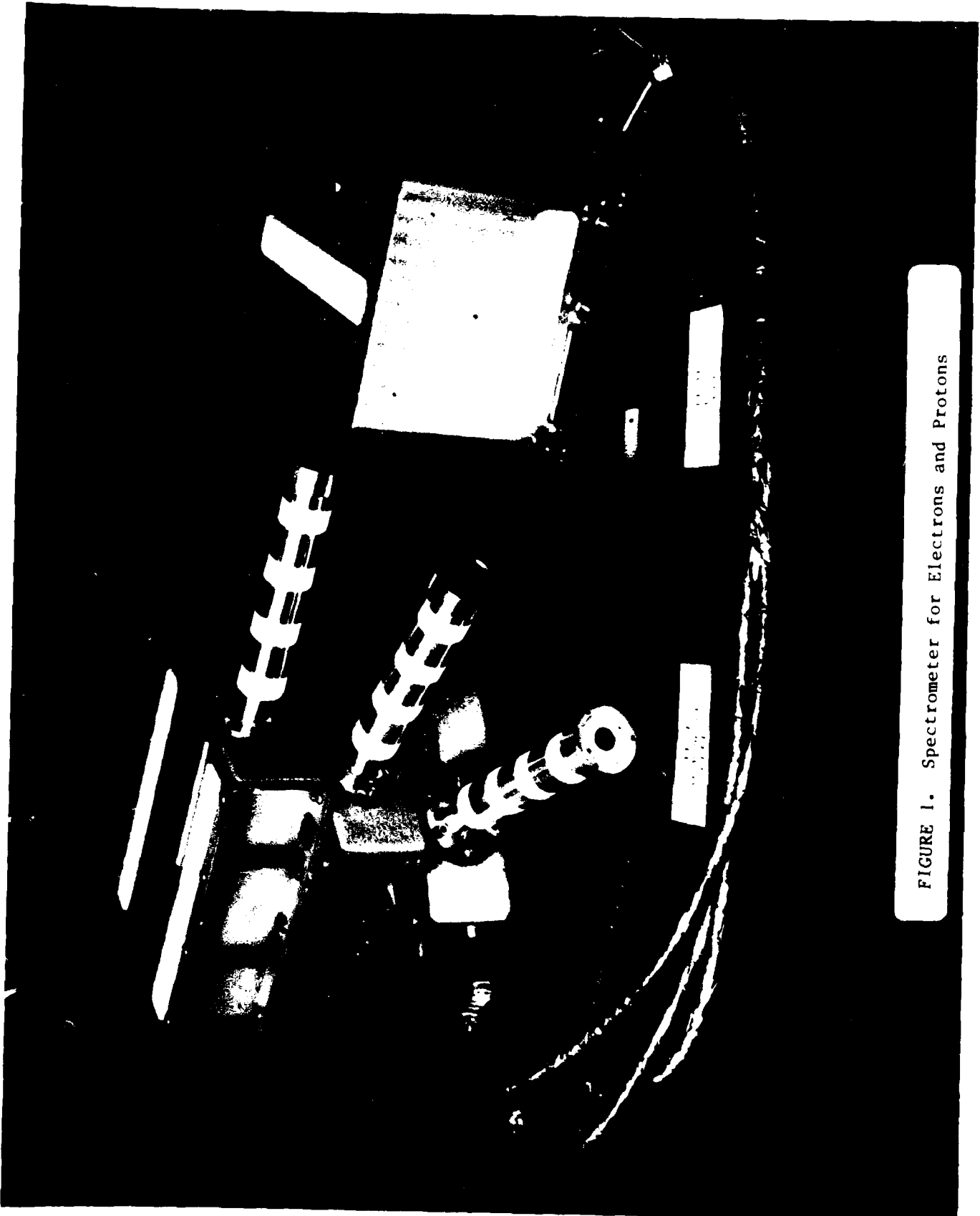


FIGURE 1. Spectrometer for Electrons and Protons

modes. In addition to the ion measurements, IMS-LO uses magnetic analyzers to measure the electron background fluxes at eight energy steps between 50 eV and 25 keV. The IMS-LO instruments are derived from the extremely productive instruments developed for the Office of Naval Research for flight on S3-3 and SCATHA. Like SC-3, the SCATHA ion mass spectrometer (SC-8) continues to operate flawlessly at this time. Figure 2 shows one of the two IMS-LO instruments. The three large circular openings are the entrance apertures to the ion collimators. Four smaller cylindrical electron collimators are visible on the right.

The Medium Energy Ion Mass Spectrometer (IMS-HI), designated ONR-307-8-3, measures ion composition in the energy range  $EM/q^2 = 20 - 8000 \text{ keV-AMU/e}^2$ . The instrument is a novel design based on ion momentum separation in a magnetic field. The ions are dispersed onto an array of six passively cooled silicon solid state detectors. Energy and mass defect analysis are performed in parallel processing electronics, allowing simultaneous measurements by each of the detectors. The instrument can be operated in two basic modes, providing full mass coverage every eight seconds or sampling of four selected ions every half second. Figure 3 shows the IMS-HI instrument. The top part of the instrument comprises the ion optics, detectors, and radiator surfaces (the square hole on the left of the figure is the entrance aperture). The bottom portion is processing electronics.

The measurement capabilities of the ONR-307 payload are summarized in Table 1.

TABLE 1: ONR-307 PAYLOAD SUMMARY

| <u>Instrument</u>       | <u>Measured Quantity</u>     | <u>Energy</u>                                 | <u>Sensor Angle to<br/>Spacecraft Spin<br/>Axis</u> |
|-------------------------|------------------------------|---|---|
| ONR-307-3<br>SEP        | Electrons<br>Protons         | 20 - 5000 keV<br>0.5 - 100 MeV                | 40°, 60°, 80°                                       |
| ONR-307-8-1,2<br>IMS-LO | Ion Composition<br>Electrons | $E/q = 0.1 - 32 \text{ keV}$<br>0.05 - 25 keV | 45°, 75°  |
| ONR-307-8-3             | Ion Composition              | $EM/q^2 = 20 - 800 \text{ keV-AMU/e}^2$       | 75°   |



FIGURE 2. Low Energy Ion Mass Spectrometer

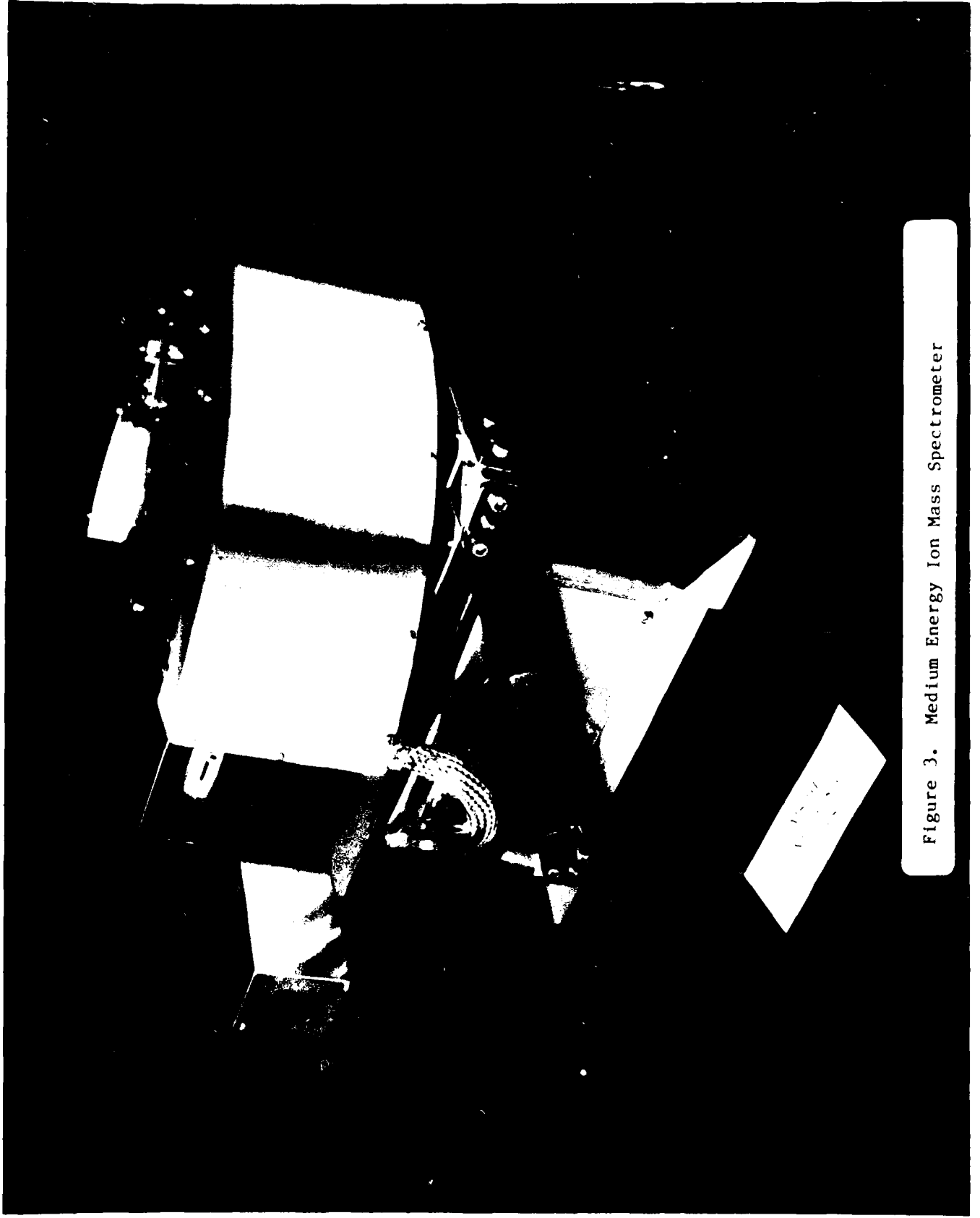


Figure 3. Medium Energy Ion Mass Spectrometer

Some of the specific tasks performed in support of the ONR-307 payload development are described below. Descriptions of EPIC payload conformance with spacecraft interface and testing requirements (e.g. thermal vacuum, vibration and electromagnetic compatibility tests) have been provided in a series of documents during the instrument development phase. A summary of payload compliance with requirements and references to the appropriate documents are given in the Statement of Conformance for ONR-307 Payload, (LMSC/F067883), which is attached as Appendix D.

Thorough electrical, mechanical, thermal, and environmental specifications have been developed and provided in support of assuring a satisfactory interface with the spacecraft and successful operation of the integrated system. These specifications are detailed in the Interface Control Documents (ICD): CRRES 227 and 228. Revision E of these two documents were published in September, 1987 and January, 1988 respectively. Compliance of the payload with the ICD is documented in the ONR-307 ICD Compliance Summary (Ref. 2; included as part of Appendix D).

Detailed procedural and functional descriptions of the of the ONR-307 payload and its operation have been provided in support of the development of the Orbital Operations Handbook (OOH), (Ref. 3). A revised draft of the OOH is in preparation and is expected to be released for review in summer, 1988.

Flight qualification testing of the ONR-307 payload was performed, including pre-integration EMC, thermal vacuum, and random vibration tests. The results of these tests have been documented in Test Data Packages (Refs. 4-6). The tests were all successfully completed, with the exception of a resonance that was discovered in the ONR-307-8-3 instrument during vibration tests. A stiffer optics support shelf for the instrument has been designed and manufactured to eliminate this problem and will be installed and retested prior to re-integration of the instrument with the spacecraft. In addition to the qualification testing described above, an extensive stress/fracture analysis was performed to satisfy shuttle safety requirements (Ref. 7), and reports on ONR-307 mass properties and safety/hazards were developed (Refs. 8, 9).

The ONR-307 instruments were successfully integrated into CRRES and completed system level testing. During spacecraft EMC tests, a problem in the spacecraft grounding that was provided for ONR-307 was identified and corrected. During thermal vacuum testing of the integrated spacecraft, the ONR-307-8-1,2 instruments each executed a single uncommanded transition to High Voltage Off. Because of problems with the Ball Aerospace spacecraft test equipment, there was no tape record of the spacecraft data during either of these occurrences. We were not able to recreate the anomaly in further testing, nor was it ever been observed during thermal vacuum testing of the instruments prior to delivery. Although it seems likely that the transitions were associated with the problems in the spacecraft test equipment, we will be carefully reviewing our design and performing follow-up testing of these instruments.

Detailed calibration of the ONR-307-3 detectors was performed at Goddard Space Flight Center (electrons - 25 to 1500 keV, protons - 230 to 1500 keV) and the Harvard cyclotron (protons - 35 to 148 MeV). Details of the calibration are included in Appendix E. Calibration of the ONR-307-8 instruments will be performed in house, using our recently constructed ion calibration facility.

Detailed requirements for agency tape contents and format were provided to AFGL, which is tasked with generating the CRRES agency tapes. Several follow-up meetings have finalized these requirements and a Data Management Plan has been developed by AFGL that satisfies the needs of ONR-307 (Ref. 10).

The Air Force Satellite Control Facility (SCF), which will be responsible for commanding and monitoring of CRRES, is currently undergoing a data system modernization (DSM). Although CRRES was originally scheduled to be supported by the old system, launch delays have assured that it will be operated under DSM. We have had several meetings with SCF personnel to specify our display requirements and develop detailed formats for instrument checkout and real time operations. A set of display modes for the old system has been developed which, although satisfactory, do not provide all of the capabilities that are desired. Because of the transition to DSM, a new set of displays will have to be developed. This task will be completed during ongoing contacts with SCF personnel.

The primary advisory group to the Space Test Program on matters concerning the CRRES instruments has been the CRRES Experimenters Working Group (CEWG). We have supported all of the CEWG meetings with the goal of assuring that ONR-307 objectives will be met by the CRRES program. The 21st CEWG meeting was held in October, 1987. Following the restructuring of the CRRES mission, it became evident that the NASA and DoD participants would require a forum to resolve issues associated with their simultaneous operations. A new working group, the Flight Operations Working Group (FOWG), was formed for this purpose. The first FOWG meeting was held in May, 1988. In addition to the CEWG and FOWG meetings, we have participated in a number of review meetings and special technical meetings in support of the ONR-307 objectives.

#### SUMMARY AND FUTURE ACTIVITIES

We have designed, manufactured, and tested the ONR-307 instrument package. The instruments have been integrated with the CRRES spacecraft and tested with the integrated system. Tasks remaining to bring the instruments to full flight readiness consist of calibration activities, installation of a redesigned optics support shelf in ONR-307-8-3, installation of flight detectors, and several minor mechanical and electrical tasks. We expect to deliver the instruments for re-integration in May, 1989, with a CRESS launch anticipated in June, 1990.

## REFERENCES

1. CRRES/Spacerad Experiment Descriptions, AFGL-TR-85-0017, January 24, 1985.
2. ONR-307 ICD Compliance Summary, LMSC/F067866, July 7, 1986.
3. Orbital Operations Handbook, BASD/CRRES Doc. CRRES-711, Rev. B, December 1, 1987.
4. Electromagnetic Compatibility Test Data Package, LMSC/F067882, July 15, 1986.
5. Thermal Vacuum Test Data Package, LMSC/F067877, July 15, 1986.
6. Random Vibration Test Data Package, LMSC/F067878, July 13, 1986.
7. ONR-307 Stress/Fracture Analysis, LMSC/F018849, January 25, 1985.
8. ONR-307 Mass Properties Data Package, LMSC/F067879, July 13, 1986.
9. ONR-307 Safety/Hazard Analysis, LMSC/F067881, July 13, 1986.
10. CRRES Data Management Plan, Data Processing Task, AFGL TM-130, June, 1986.

APPENDIX A

#### Contents

|                           |    |
|---------------------------|----|
| 1. Scientific Objectives  | 87 |
| 2. Application            | 88 |
| 3. Measuring Techniques   | 89 |
| 4. Function Block Diagram | 91 |
| Acknowledgments           | 94 |
| References                | 94 |

## 9. The Spectrometer for Electrons and Protons (ONR-307-3)

by

J.B. Reagan, E.E. Gaines, S.J. Battel,  
D.A. Simpson, W.L. Imhof, and R.R. Vondrak  
Lockheed Palo Alto Research Laboratory  
Palo Alto, CA 94304

### 1. SCIENTIFIC OBJECTIVES

The ONR-307-3 Spectrometer for Electrons and Protons (SEP) measures with fine pitch-angle resolution the flux of energetic electrons in the energy range of 20-5000 keV and the flux of energetic protons in the energy range 500 keV-100 MeV. The ONR-307-3 SEP consists of three identical particle telescopes composed of surface-barrier silicon detectors with active anticoincidence shielding and narrow collimation (3° FWHM). The energy spectra are measured with fine energy resolution: 24 contiguous channels for the electrons, and 48 contiguous channels for protons. The three particle telescopes are mounted at optimum angles to the CRRES spin axis to provide nearly complete pitch-angle coverage on each spacecraft spin.

The SEP is one component of the ONR-307 Energetic Particles and Ion Composition (EPIC) Experiment. The other EPIC instruments are the ONR-307-8-1,

ONR-307-8-2 Low Energy Ion Mass Spectrometers that measure primarily the ion composition between 0.1 and 32 keV/q,<sup>1</sup> and the ONR-307-8-3 Medium Energy Ion Mass Spectrometer that measures the ion composition between 20 and 8000 keV-AMU/q.<sup>2, 2</sup>

The overall objective of the ONR-307-3 experiment is to obtain necessary data to construct predictive models, suitable for engineering purposes, of the energetic particle and plasma environment in those regions of space of primary interest to the DOD satellite operations. The specific science objectives of this experiment are:

(1) To measure the intensity, energy spectra, and pitch angle distribution of energetic electrons and protons continuously as a function of time. These measurements will characterize the dynamical behavior of the radiation belts.

(2) To compute accurately the total omnidirectional flux at the satellite position.

(3) To understand the physics of the sources, energization, transport, lifetimes, and losses of energetic particles in the Earth's radiation belts.

(4) To understand the details of wave-particle interactions (WPI), both natural and manmade, that are a principal loss mechanism for radiation belt particles. These WPI produce particle precipitation into the ionosphere that can disrupt radio-wave communications of vital interest to the U.S. Navy.

(5) To utilize this experimental data base to greatly improve the accuracy of the trapped radiation belt models and to characterize model particle precipitation.

## 2. APPLICATION

The ONR-307-3 SEP Experiment will measure continuously the complete energy and angular distribution of the energetic electrons and protons. This measurement of the complete distribution of the trapped energetic particle population with fine angular resolution is necessary to:

(a) "Remote sense" the omnidirectional flux far away from the satellite orbit plane by directly unfolding the measured in situ pitch angle distribution to derive the pitch angle distribution at all lower altitudes. A measurement of the complete pitch angle distribution at the CRRES satellite enables the experimenter, through adiabatic transformation of the particle bounce motion, to define the particle popu-

1. Quinn, J.M., Shelley, E.G., Battel, S.J., Hertzberg, E., Roselle, S., and Saunders, T.C. (1985) The Low Energy Ion Mass Spectrometer (ONR-307-8-1, ONR-307-8-2), AFGL-TR-85-0017 (this volume).
2. Voss, H.D., Shelley, E.G., Ghielmetti, A.G., Hertzberg, E., Battel, S.J., Appert, K.L., and Vondrak, R.R. (1985) The Medium Energy Ion Mass Spectrometer (IMS-HI) (ONR-307-8-3), AFGL-TR-85-0017 (this volume).

lation on the field line below the satellite. Such measurements are absolutely essential to the mapping of the radiation belts to all altitudes.

(b) Investigate the narrow "source/loss cone" regions of the pitch angle distribution that are the primary sources and the major sinks of radiation belt particles. The pitch angle diffusion of particles into the atmospheric loss cone is one of the principal mechanisms for radiation belt depletion. Understanding the pitch angle diffusion rates into the loss cone caused by natural and manmade waves is central to modeling the dynamic behavior of the radiation belts.

The ONR-307-3 instrument can accomplish these objectives because it has comprehensive pitch angle measurements with fine angular resolution ( $3^\circ$  FWHM). The arrangement of the three identical telescopes, combined with the spin of the spacecraft, will provide nearly complete measurement of the particle distribution function for all orientations of the spin axis to the magnetic field.

High temporal resolution measurements (0.25 sec) will enable the study of source/loss cone transient mechanisms, substorm injections, and L-shell splitting. A 12-channel energy spectrum is obtained every 0.25 sec. The pitch angle distribution from  $0$  to  $90^\circ$  over 12 energy channels is obtained every 7.5 sec at a spin rate of 2 rpm. Complete angular distribution functions over the entire energy range for both electrons (24 energy channels) and protons (48 energy channels) can be obtained in about 3 min.

### 3. MEASURING TECHNIQUES

The ONR-307-3 instrument is based heavily on the successful SC-3 spectrometer on the SCATHA mission and consists of a series of solid-state particle spectrometers, each with four detector elements. The SC-3 instrument was described in detail by Reagan et al.<sup>3</sup> and by Stevens and Vampola.<sup>4</sup> The configuration of each spectrometer is shown in Figure 26. Various logic combinations of the four detector elements in the spectrometer determine the particle types and energy ranges that are measured in several command-selectable, time-multiplexed modes of operation.

The D-detector, 200- $\mu\text{m}$  thick intrinsic Si, measures both the rate of energy loss of the higher energy particles, and directly stops and measures the lower en-

3. Reagan, J.B., Nightingale, R.W., Gaines, E.E., Imhof, W.L., and Stassinopoulos, E.G. (1981) Outer zone energetic electron spectral measurements, *J. Spacecraft and Rockets* 18:83-88.
4. Stevens, J.R., and Vampola, A.L. (1978) *Description of the Space Test Program P78-2 Spacecraft and Payloads*, Space and Missile Systems Organization, Air Force Systems Command, TR-78-24.

ergy particles. The E-detector, a stack of five 2-mm-thick detectors in parallel, is located behind the D-detector to stop the higher energy particles and to measure their total energy loss. The E'-detector, 1000  $\mu\text{m}$  thick, is located behind the E-detector and is used as an active collimator. Behind the E'-detector is a tungsten absorber that sets the upper energy limit for analysis.

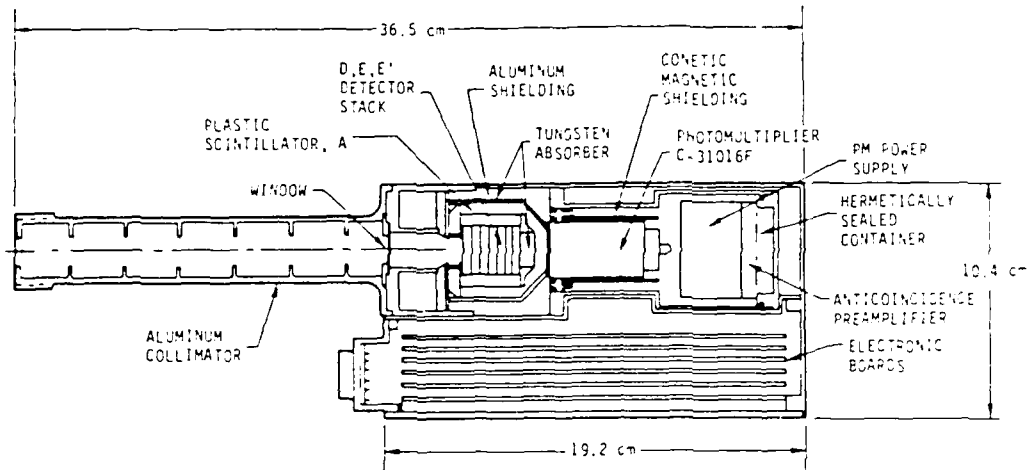


Figure 26. Cross-Section View of the SCATHA SC-3 Energetic Electron/Proton Spectrometer Showing the Various Sensor Elements and the Long Collimator

All of these detectors are fabricated of surface-barrier silicon and are stacked together in a telescope configuration. The entire stack is surrounded by the A-anticoincidence detector, a plastic scintillator viewed by a photomultiplier tube. The A-detector senses and rejects energetic particles and bremsstrahlung that penetrate either the outer shielding walls of aluminum and tungsten or the silicon detector stack and absorber. The detector stack is located behind a long, narrow collimator that defines the  $3^\circ$  angular field-of-view (FWHM). The instrument geometric factor is approximately  $3 \times 10^{-3} \text{ cm}^2\text{-ster.}^3$

Three spectrometers are oriented at angles of  $80^\circ$ ,  $60^\circ$ , and  $40^\circ$  to the CRRES spin axis. These three spectrometers comprise the ONR-307-3-1 Sensor Package (SP) shown in Figure 27. The instrument analyzer electronics are mounted near the SP in the ONR-307-3-2 Analyzer Package (AP); both units are mounted on the

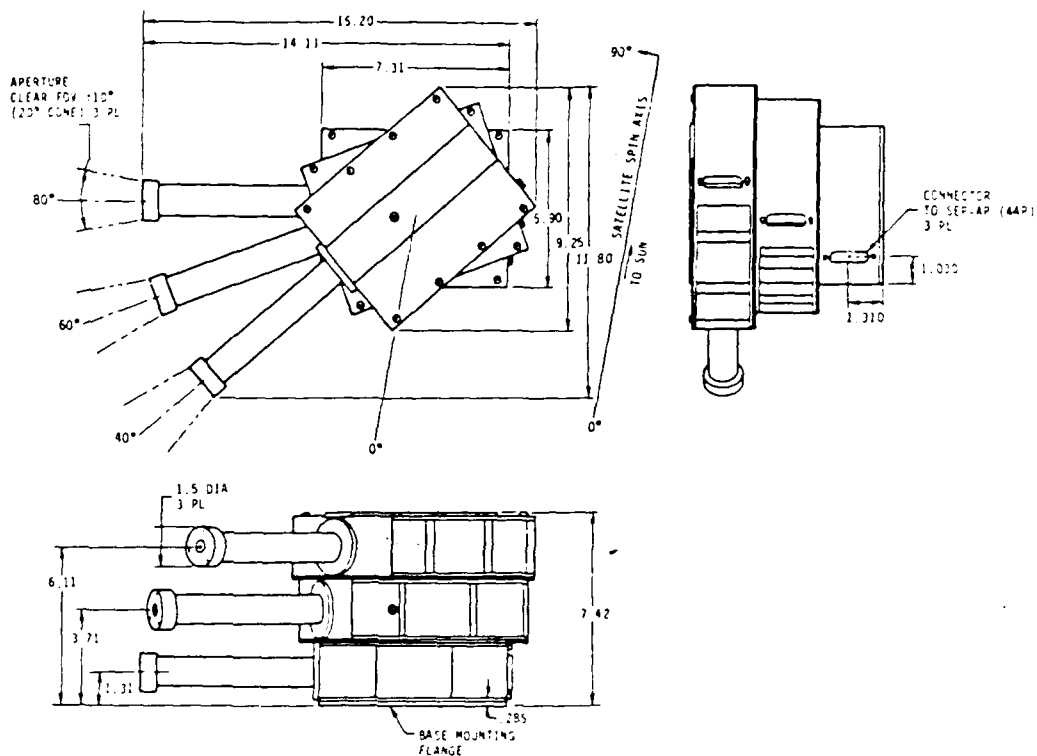


Figure 27. Mechanical Arrangement of the Three SEP Telescopes

bottom of the spacecraft. The AP and SP are separated to achieve a lower temperature in the silicon detectors for improved low-energy electron detection.<sup>5, 6</sup>

#### 4. FUNCTION BLOCK DIAGRAM

A function block diagram of the ONR-307-3 instrument is shown in Figure 28. The instrument operates from a CMOS memory of 768 8-bit words that are individually addressable and loadable via a 16-bit serial-digital command. Twelve of these words (32-bit control register for each of the three sensors) completely

5. Voss, H.D., Reagan, J.B., Imhof, W.L., Murray, D.O., Simpson, D.A., Cauffman, D.P., and Bakke, J.C. (1982a) Low temperature characteristics of solid state detectors for energetic X-ray, ion and electron spectrometers, IEEE Trans. Nucl. Sci. NS-29:164.
6. Voss, H.D., Bakke, J.C., and Roselle, S.N. (1982b) A spacecraft multichannel analyzer for a multidetector solid state detector array, IEEE Trans. Nucl. Sci. NS-29:173.



define one operating MODE of the instrument. A MODE is defined by specifying the logic conditions (coincidence/anticoincidence), gain, and energy thresholds required between the four detector elements (D, E, E', A) to uniquely establish a particle type and energy range for analysis. A choice of two amplifier gain settings for the D- and E-detectors is available. The lower and upper energy thresholds selected for analysis by the 12-channel pulse height analyzer (PHA) are determined to 8- and 6-bit resolution, respectively. Either the D- or E-detector is selectable at any time for analysis by the PHA through the multiplexer. The energy threshold of the sensor not selected for analysis can be set to 8-bit resolution.

The operating modes can be structured to emphasize one particle type, such as electrons, or all particle types; to concentrate on special events, such as solar particle events; or to dwell on a narrow energy region of interest with any particle type. The commandable options are extensive, but an optimum operating configuration will be loaded initially and adjusted as conditions dictate. A hard-wired backup MODE can be selected if a major failure occurs in the memory operation. The hard-wired backup MODE measures the higher energy electrons (300-5100 keV) and is independent of the memory. The instrument operates in this condition automatically whenever the memory is being loaded or disabled.

The operating modes will be selected as required to optimize data collection in the inner and outer radiation belts. The basic programmable mode parameters are the energy range and energy channel widths for the electrons and for the protons. Typical modes that may be used during the CRRES mission are shown in Table 13.

Table 13. Spectrometer for Electrons and Protons: Typical Operating Modes

| Species   | Mode  | Energy Range | Channel Width |
|-----------|-------|--------------|---------------|
| Electrons | ELEC1 | 20-300 keV   | 20 keV        |
|           | ELEC2 | 300-5000 keV | 400 keV       |
| Protons   | PROT1 | 0.5-4.5 MeV  | 330 keV       |
|           | PROT2 | 4.5-20 MeV   | 1.25 MeV      |
|           | PROT3 | 20-45 MeV    | 2.0 MeV       |
|           | PROT4 | 45-100 MeV   | 4.2 MeV       |

## Acknowledgments

The authors wish to thank J.C. Bakke, L.A. Hooker, and V.F. Waltz for their efforts in the design, development, and fabrication of this instrument. We also deeply appreciate the assistance of our co-investigator, H.D. Voss.

This work was supported by the Office of Naval Research under contract N00014-83-C-0476 and by the Lockheed Independent Research Program.

## References

1. Quinn, J.M., Shelley, E.G., Battel, S.J., Hertzberg, E., Roselle, S., and Saunders, T.C. (1984) The Low Energy Ion Mass Spectrometer (ONR-307-8-1, ONR-307-8-2), AFGL-TR-85-0017 (this volume).
2. Voss, H.D., Shelley, E.G., Ghielmetti, A.G., Hertzberg, E., Battel, S.J., Appert, K.L., and Vondrak, R.R. (1984) The Medium Energy Ion Mass Spectrometer (IMS-HI) (ONR-307-8-3), AFGL-TR-85-0017 (this volume).
3. Reagan, J.B., Nightingale, R.W., Gaines, E.E., Imhof, W.L., and Stassinopoulos, E.G. (1981) Outer zone energetic electron spectral measurements, J. Spacecraft and Rockets 18:83-88.
4. Stevens, J.R., and Vampola, A.L. (1976) Description of the Space Test Program P78-2 Spacecraft and Payloads, Space and Missile Systems Organization, Air Force Systems Command, TR-78-24.

5. Voss, H.D., Reagan, J.B., Imhof, W.L., Murray, D.O., Simpson, D.A., Cauffman, D.P., and Bakke, J.C. (1982a) Low temperature characteristics of solid state detectors for energetic X-ray, ion and electron spectrometers, IEEE Trans. Nucl. Sci. NS-29:164.
6. Voss, H.D., Bakke, J.C., and Roselle, S.N. (1982b) A spacecraft multichannel analyzer for a multidetector solid state detector array, IEEE Trans. Nucl. Sci. NS-29:173.

APPENDIX B

Contents

|                           |     |
|---------------------------|-----|
| 1. Scientific Objectives  | 141 |
| 2. Applications           | 142 |
| 3. Measuring Techniques   | 143 |
| 4. Function Block Diagram | 149 |
| Acknowledgments           | 149 |
| References                | 151 |

15. The Low Energy Ion Mass Spectrometer  
(ONR-307-8-1, 307-8-2)

by

J.M. Quinn, E.G. Shelley, S.J. Battel,  
E. Hertzberg, S. Roselle, and T.C. Sanders  
Lockheed Palo Alto Research Laboratory  
Palo Alto, CA 94304

1. SCIENTIFIC OBJECTIVES

The Low Energy Ion Mass Spectrometer (IMS-LO) is designed to measure plasmas that are the sources of radiation belt particles, and to provide data on the origin and acceleration processes of these plasmas. To achieve these objectives, the IMS-LO measures energy and mass spectra covering the ranges of  $E/q = 0.1 - 32 \text{ keV/e}$  and  $M/q$  from  $<1$  to  $>30 \text{ AMU/e}$  with good coverage of pitch angles throughout the orbit.

These data will be used to investigate plasma interaction processes including: (1) the plasma and field conditions that produce ionospheric acceleration, precipitation of energetic particles from the trapped populations, and very-low frequency (vlf) wave generation and amplification; (2) the local time and invariant latitude distributions of ionospheric ion source regions; and (3) the large-scale and small-scale transport and energization processes for the hot plasmas.

## 2. APPLICATIONS

A series of spacecraft instrumented to measure plasma composition has yielded important results from a wide variety of magnetospheric locations. One of these was the S3-3 satellite, launched in July 1976, that led to the discovery of intense upflowing ionospheric ions at altitudes near  $1 R_E$  and the determination of the morphology of these flows. Increase in the ionospheric component of trapped keV ring current ions with storm activity was also established with these data. The S3-3 results are reviewed by Sharp et al.<sup>1</sup>

Following S3-3, plasma composition measurements were made on GEOS-1, launched in April 1977 into an eccentric equatorial orbit;<sup>2</sup> ISEE-1, launched in October 1977;<sup>3,4</sup> GEOS-2, launched into geosynchronous orbit in July 1978;<sup>2</sup> PROGNOZ-7, launched into a highly eccentric orbit with 65° inclination in October 1978;<sup>5</sup> SCATHA, launched into a near-geosynchronous orbit in January 1979;<sup>4,6</sup> DE-1, launched into a polar eccentric orbit with apogee of  $4.6 R_E$  in August 1981;<sup>7</sup>

1. Sharp, R.D., Ghielmetti, A.G., Johnson, R.G., and Shelley, E.G. (1983a) Hot plasma composition results from the S3-3 spacecraft, in Energetic Ion Composition in the Earth's Magnetosphere, R.G. Johnson, Ed., TERRAPUB, Tokyo.
2. Balsiger, H., Geiss, J., and Young, D.T. (1983) The composition of thermal and hot ions observed by the GEOS-1 and -2 spacecraft, in Energetic Ion Composition in the Earth's Magnetosphere, R.G. Johnson, Ed., TERRAPUB, Tokyo.
3. Sharp, R.D., Johnson, R.G., Lennartsson, W., Peterson, W.K., and Shelley, E.G. (1983b) Hot plasma composition results from the ISEE-1 spacecraft, in Energetic Ion Composition in the Earth's Magnetosphere, R.G. Johnson, Ed., TERRAPUB, Tokyo.
4. Horowitz, J.L., Chappell, C.R., Reasoner, D.L., Craven, P.D., Green, J.L., and Baugher, C.R. (1983) Observations of low-energy plasma composition from the ISEE-1 and SCATHA satellites, in Energetic Ion Composition in the Earth's Magnetosphere, R.G. Johnson, Ed., TERRAPUB, Tokyo.
5. Lundin, R., Hultqvist, B., Pissarenko, N., and Zachorov, A. (1983) Composition of hot magnetospheric plasma as observed with the PROGNOZ-7 satellite, in Energetic Ion Composition in the Earth's Magnetosphere, R.G. Johnson, Ed., TERRAPUB, Tokyo.
6. Johnson, R.G., Strangeway, R.J., Shelley, E.G., Quinn, J.M., and Kaye, S.M. (1983) Hot plasma composition results from the SCATHA spacecraft, in Energetic Ion Composition in the Earth's Magnetosphere, R.G. Johnson, Ed., TERRAPUB, Tokyo.
7. Shelley, E.G., Balsiger, H., Eberhardt, P., Geiss, J., Ghielmetti, A., Johnson, R.G., Peterson, W.K., Sharp, R.D., Whalen, B.A., and Young, D.T. (1983) Initial hot plasma composition results from the Dynamics Explorer, in Energetic Ion Composition in the Earth's Magnetosphere, R.G. Johnson, Ed., TERRAPUB, Tokyo.

and AMPTE/CCE, launched into an eccentric low latitude ( $\sim 5^\circ$ ) orbit with apogee of  $8.8 R_E$  in August 1984.<sup>8</sup>

The contributions of these instruments are too numerous to list here; however, the plasma composition of a large number of magnetospheric regions has now been examined. The data show intricate dependences on local time, radial distance, pitch angle, energy, magnetic storm and substorm activity, and solar cycle. Sufficient information about the plasma morphology and dynamics have been obtained to make an excellent starting point for the modeling goals of CRRES.

Determining the behavior of different ion species in the energy range covered by the IMS-LO instruments is critical to the development of detailed ring current models. A thorough understanding of ring current dynamics will require detailed knowledge of the particle source contributions, transport phenomena, energization processes, and, finally, scattering and loss mechanisms. Although initial attempts to model ring current dynamics cannot await such a comprehensive understanding, the basic components of source, transport, and loss must be represented as accurately as possible. Ion composition data are essential for determining total ion energy density (ring current) and they provide a necessary link in modeling the life of ring current ions.

### 3. MEASURING TECHNIQUES

The IMS-LO-1 and IMS-LO-2 instruments rely upon the same design that was successfully implemented with previous Lockheed instruments on SCATHA (launched January 1979) and S3-3 (launched July 1976). Each version of the instrument has had improved range of coverage, resolution and operating flexibility.

IMS-LO-1 and IMS-LO-2 are identical instruments mounted at  $45^\circ$  and  $75^\circ$  to the spacecraft spin axis to maximize coverage of fluxes near the magnetic field line direction. Each instrument performs ion composition measurements in the energy per charge range 0.1-32 keV/e and the mass per charge range  $<1$  to  $>32$  AMU/e. The energy range is broken into three contiguous parts, each consisting of 15 energy steps, a coverage of 45 energy steps in all. The three portions of the energy coverage are sampled in parallel by three separate analyzer and sensor heads. After each 15-step sequence, the background counting rate is measured for each sensor head. The mass range ( $<1$  to  $>32$  AMU/e) is covered by 32 steps. Alternatively, the spectrometer can be commanded to sample the high mass range above 16 AMU/e. In addition to ion measurements, each of the two

8. Shelley, E.G., Ghielmetti, A., Hertzberg, E., Battel, S.J., Altwegg-Von Burg, K., and Rulsiger, H. (1984) AMPTE/CCE hot plasma composition experiment (HPCE), submitted to IEEE Trans. Remote Sensing.

instruments monitors the background electron flux at four fixed energies. The electron channels are described in Section 3.1.

### 3.1 Ion Optics

Each of the IMS-LO instruments consists of three parallel analyzer units (or heads) which measure ions in a different portion of the  $E/q$  range from 0.1 - 32 keV/e. One of the analyzer heads is illustrated in Figure 45. Collimated ions enter a crossed electric and magnetic field velocity filter (Wein Filter), pass through an angle-focusing, hemispherical sector, electrostatic analyzer, and are detected by a channel electron multiplier. Details of the optics system follow.

Ions enter the instrument through a collimator with an acceptance cone of approximately  $5^\circ$  full width. Following collimation, the ions enter the crossed electric and magnetic field velocity filter, which, in conjunction with the electrostatic energy analysis, acts as the mass analyzer (MA). The MA consists of a fixed magnetic field and a crossed electric field that is varied according to the value of  $E/q$  and  $M/q$  being sampled. The fields are oriented so that the electric and magnetic forces on an ion are in opposition, and the electric field is chosen so that there is no net force on an ion of the desired mass and energy, allowing it to pass through the MA in a straight trajectory. The MA magnetic field values in the three heads are nominally fixed at 445, 1211, and 3304G. The electric field plates of the MA are driven symmetrically and the voltages for a given mass selection scale as the square root of the ion energy as determined by the voltage applied to the electrostatic analyzer (EA) discussed later in this section. The maximum MA plate potentials in the three heads, corresponding to the minimum value of  $M/q$  and the maximum value of  $E/q$  sampled within each head, are nominally  $\pm 35$ ,  $\pm 253$ , and  $\pm 1850$  V for the normal mass range and a factor of four lower for the heavy ion mode. The three heads are driven by a common high voltage power supply and voltage divider network that provides the different ranges required.

Following the velocity filter, ions are bent  $180^\circ$  in a spherical sector EA that is angle focusing and energy dispersive. As with the MA, the EA plates in the three heads are driven by a common power supply and voltage divider network. The ratio between consecutive values of the logarithmically spaced energy steps is approximately 1.14, and there are 15 energy steps within each head. Thus, the values of  $E/q$  simultaneously sampled by the three heads are spaced by a factor of approximately seven, with the first head covering from 0.1 - 0.6 keV/e, the second from 0.7 - 4.5 keV/e, and the third from 5 - 32 keV/e. The EA plate separation in the high energy head is reduced from that of the other two heads to achieve the desired energy range without excessively high voltages. After exiting the EA, ions are post-accelerated and enter the channel electron multiplier.

# WEIN FILTER ION MASS SPECTROMETER

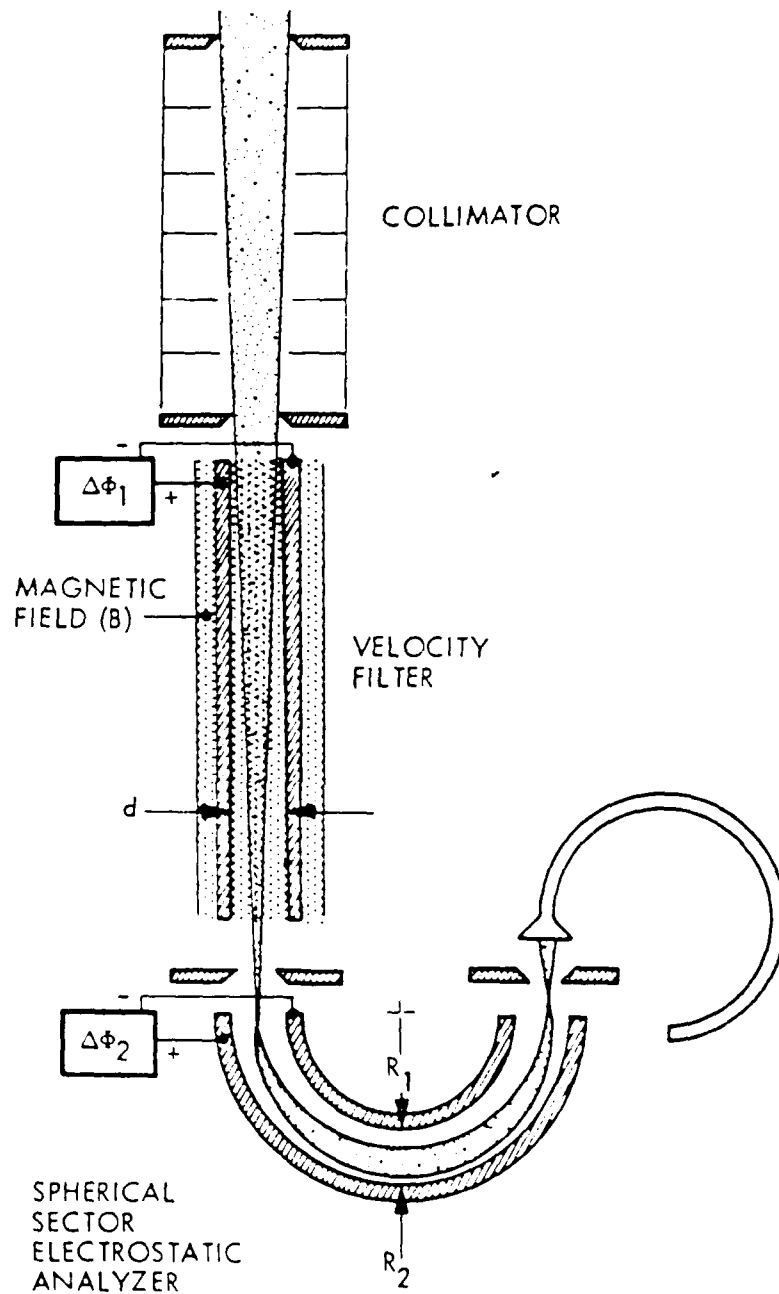


Figure 45. Schematic Illustration of Ion Mass and Energy Analysis Optics for the Low Energy Ion Mass Spectrometer (IMS-LO)

Figure 46 shows peak shapes obtained from the Lockheed mass spectrometer on S3-3. The open circles with error bars are on-orbit data; the dashed line represents inferred peak shapes. Separation of the species is quite good.

The coordinated stepping of the EA and MA is done under digital control in a number of modes as described in Section 3.2. Each sample of a particular mass-energy value requires 64 ms. A 12-ms deadtime at the beginning of each sampling period ensures complete settling of the analyzer power supplies.

Each of the three heads measures background counts in "Energy Step 0," an additional step to the 15 energy steps described above. The background measurement is performed by disabling the MA power supply and setting the EA power supply to step 4. As the MA power supply decays toward zero, the analyzers pass continually higher masses. Following the 12-ms deadtime, the background channel is sampling M/q values well above the ambient ion mass peaks and measures

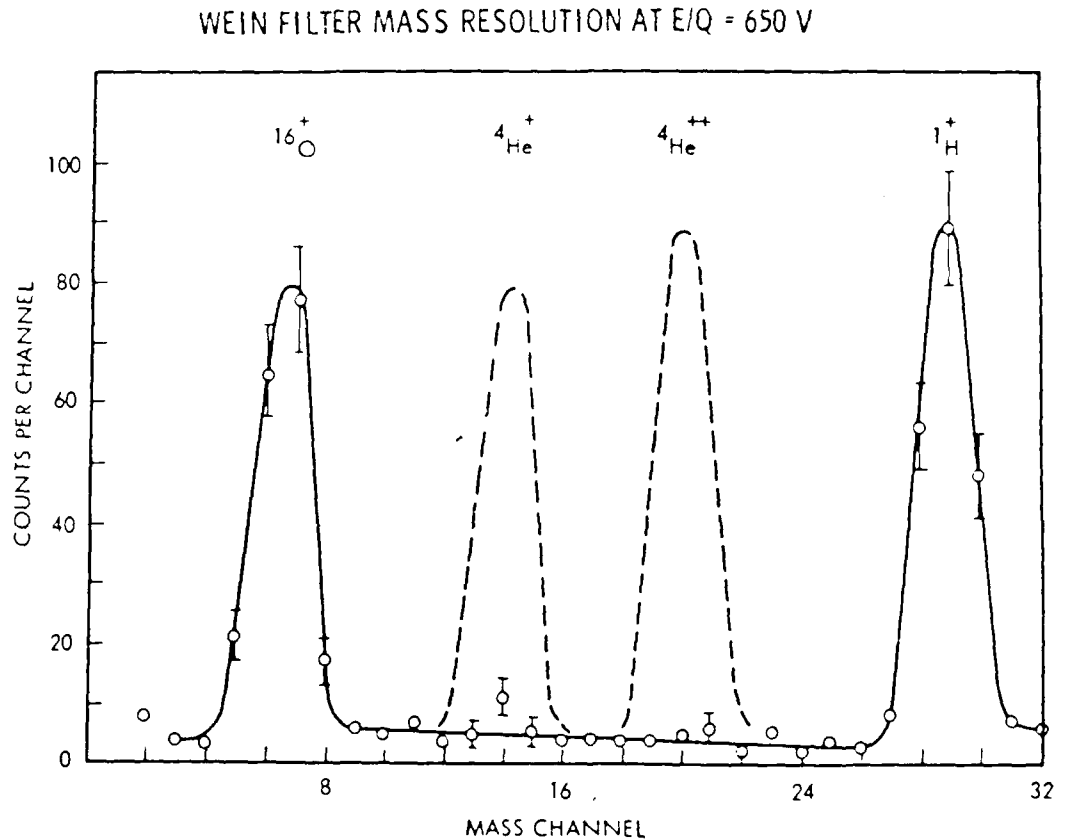


Figure 46. Mass Peak Shapes for the Wein Filter Spectrometer

the instrument background response only. The instrument geometric factors are approximately  $4 \times 10^{-4} \text{ cm}^2\text{-ster}$  for the two low energy heads and about one-half this value for the high energy head.  $\Delta E/E$  is approximately 10 percent.

### 3.2 Operating Modes

The two basic submodes of operation are SWEEP and LOCK. In LOCK mode, the instrument locks onto a particular  $M/q$  value while stepping in energy. Each of the 15 energy values and background are sampled for 64 ms in each of the three heads, giving a 45-point energy spectrum for a particular species in 1.024 seconds (approximately  $12^\circ$  of spacecraft rotation). The LOCK submode obtains 32 consecutive energy spectra at a fixed mass value (approximately one spacecraft rotation) before moving into the next submode.

In SWEEP submode, the instrument sequentially "sweeps" through the 32-step mass range at each of the 15 energy steps and background. A mass sweep at one energy step requires 2.084 seconds. The entire 32.768-second SWEEP submode obtains a complete sampling of the 32 by 48 mass-energy array (32 by 16 in each of the three heads). As in the LOCK submode, 3 of the 48 energy points are actually background measurements (1 in each head).

The duration of each of the submodes is 32.768 seconds, approximately one spacecraft spin. The submodes may be combined to form the three basic modes of operation: LOCK-ONLY, SWEEP-ONLY, and SWEEP-LOCK. As the names imply, LOCK-ONLY consists only of LOCK submodes, SWEEP-ONLY of SWEEP submodes, and SWEEP-LOCK alternates between SWEEP and LOCK. In either the LOCK-ONLY or SWEEP-LOCK modes, the mass channels used for the LOCK submode are sequentially executed from four values commanded into the instrument memory. These values may select any 4 of the 32  $M/q$  steps corresponding to any four ion species, for instance,  $\text{H}^-$ ,  $\text{He}^-$ ,  $\text{He}^{++}$ ,  $\text{O}^-$ , or  $\text{H}^-$ ,  $\text{O}^-$ ,  $\text{H}^-$ ,  $\text{O}^-$ ; or  $\text{O}^-$ ,  $\text{O}^-$ ,  $\text{O}^+$ ,  $\text{O}^+$ . IMS-LO-1 and IMS-LO-2 are commanded independently so that the two instruments can operate in different modes simultaneously.

In addition to the normal range of mass coverage, the instrument can be commanded into a Heavy Ion Mode. In this mode, the MA voltages are reduced by a factor of 4, scaling the  $M/q$  coverage upward by a factor of 16.

### 3.3 Electron Detectors

Each of the IMS-LO instruments contains a set of four broadband, fixed-energy electron detectors that monitor electron fluxes between 50 eV and 25 keV. The  $\Delta E/E$  for each detector is 50 percent and the central energies of the four electron channels on IMS-LO-1 and IMS-LO-2 are interleaved, providing a total of eight

channels with central energies from 0.067 to 20 keV. The electron detectors accumulate for 512 ms, providing samples approximately every 6° of spacecraft spin.

Figure 47 schematically illustrates the electron optics for one of the eight detectors. Entering electrons are collimated to a 5° acceptance cone and pass through an aperture that sets the geometric factor. The electrons are then bent

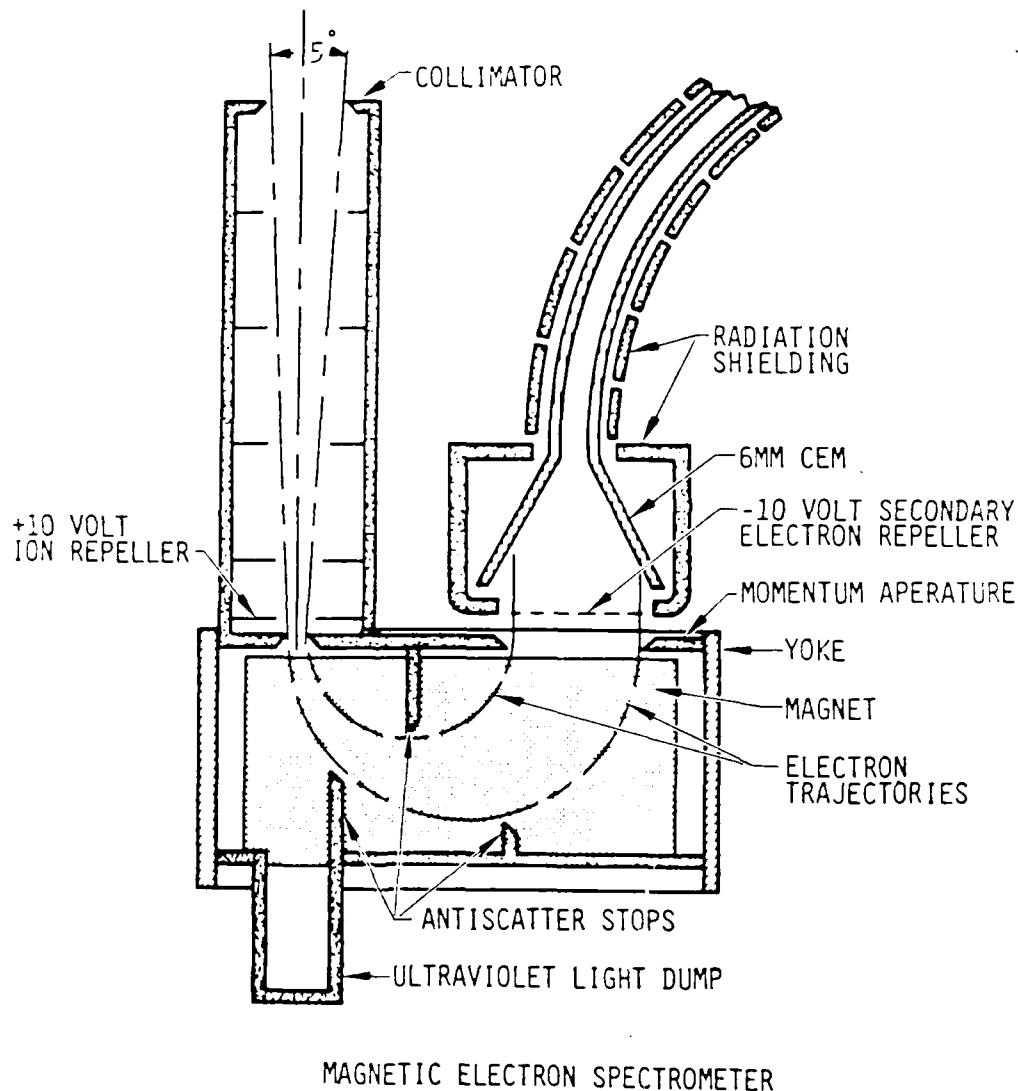


Figure 47. Schematic Illustration of the Electron Detector for the Low Energy Ion Mass Spectrometer (IMS-LO)

180° in a magnetic analyzer and pass through an exit aperture that sets  $\Delta E/E$  before entering the channeltron sensor.

#### 4. FUNCTION BLOCK DIAGRAM

The block diagram shown in Figure 48 illustrates the flow of data through the instrument. Counts from the preamp/discriminators increment 15-bit accumulators. Data from the accumulators are read into buffers every 64 ms for ions and every 512 ms for electrons. These data are then log compressed into 8 bits and are sequentially fed into the data stream.

The discriminator threshold for each sensor is set by command to one of four values. A special calibration cycle may be commanded that sequentially steps through the four thresholds while remaining locked on a selected mass step. In addition, the calibration command may optionally enable a pulser that checks each preamp/discriminator and accumulator by injecting pulses at a fixed rate.

The channel electron multiplier bias is command selectable to one of four values to compensate for possible channel multiplier gain degradation. The gain of each channel electron multiplier is periodically determined via the calibration cycle described above.

#### Acknowledgments

The authors wish to express their appreciation to J. C. Bakke, L. A. Hooker, and V. F. Waltz for their efforts in the design, development, and fabrication of this instrument. We are also deeply indebted to our co-investigators, R. G. Johnson, R. D. Sharp, and R. R. Vondrak for making this instrument (and its predecessors) possible.

This effort was supported by the Office of Naval Research under contract N00014-83-C-0476 and by the Lockheed Independent Research Program.

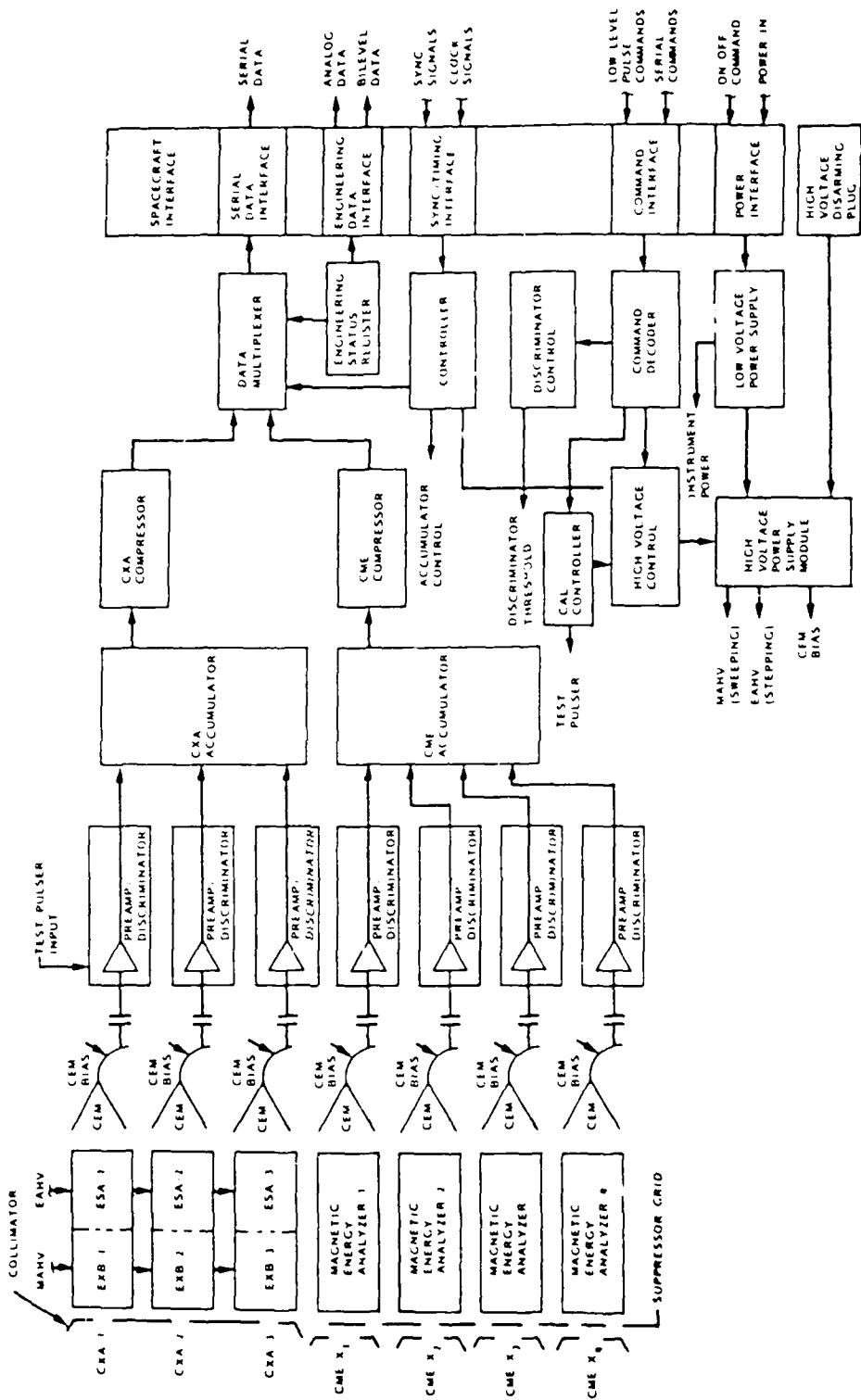


Figure 43. Function Block Diagram for One of the Two Identical Low Energy Ion Mass Spectrometers (IMS-1.0)

## References

1. Sharp, R.D., Ghielmetti, A.G., Johnson, R.G., and Shelley, E.G. (1983a) Hot plasma composition results from the S3-3 spacecraft, in Energetic Ion Composition in the Earth's Magnetosphere, R.G. Johnson, Ed., TERRAPUB, Tokyo.
2. Balsiger, H., Geiss, J., and Young, D.T. (1983) The composition of thermal and hot ions observed by the GEOS-1 and -2 spacecraft, in Energetic Ion Composition in the Earth's Magnetosphere, R.G. Johnson, Ed., TERRAPUB, Tokyo.
3. Sharp, R.D., Johnson, R.G., Lennartsson, W., Peterson, W.K., and Shelley, E.G. (1983b) Hot plasma composition results from the ISEE-1 spacecraft, in Energetic Ion Composition in the Earth's Magnetosphere, R.G. Johnson, Ed., TERRAPUB, Tokyo.
4. Herowitz, J.L., Chappell, C.R., Reasner, D.L., Craven, P.D., Green, J.L., and Baugher, C.R. (1983) Observations of low-energy plasma composition from the ISEE-1 and SCATHA satellites, in Energetic Ion Composition in the Earth's Magnetosphere, R.G. Johnson, Ed., TERRAPUB, Tokyo.
5. Lundin, R., Hultqvist, B., Pissarenko, N., and Zacharov, A. (1983) Composition of hot magnetospheric plasma as observed with the PROGNOZ-7 satellite, in Energetic Ion Composition in the Earth's Magnetosphere, R.G. Johnson, Ed., TERRAPUB, Tokyo.
6. Johnson, R.G., Strangeway, R.J., Shelley, E.G., Quinn, J.M., and King, S.M. (1983) Hot plasma composition results from the SCATHA spacecraft, in Energetic Ion Composition in the Earth's Magnetosphere, R.G. Johnson, Ed., TERRAPUB, Tokyo.
7. Shelley, E.G., Balsiger, H., Eberhardt, F., Geiss, J., Ghielmetti, A., Johnson, R.G., Peterson, W.K., Sharp, R.D., Whalen, B.A., and Young, D.T. (1983) Initial hot plasma composition results from the Dynamics Explorer, in Energetic Ion Composition in the Earth's Magnetosphere, R.G. Johnson, Ed., TERRAPUB, Tokyo.
8. Shelley, E.G., Ghielmetti, A., Hertzberg, E., Battel, S.J., Altwegg-Von Burg, K., and Balsiger, H. (1984) AMPTE/CCE hot plasma composition experiment (HPCE), submitted to IEEE Trans. Remote Sensing.

APPENDIX C

## Contents

|                           |     |
|---------------------------|-----|
| 1. Scientific Objectives  | 153 |
| 2. Applications           | 154 |
| 3. Measuring Techniques   | 155 |
| 4. Function Block Diagram | 158 |
| Acknowledgments           | 158 |
| References                | 160 |

## 16. The Medium Energy Ion Mass Spectrometer (ONR-307-8-3)

by

H.D. Voss, E.G. Shelley, A.G. Ghielmetti, E. Hertzberg,  
S.J. Battel, K.L. Appert, and R.R. Vondrak  
Lockheed Palo Alto Research Laboratory  
Palo Alto, CA 94304

### I. SCIENTIFIC OBJECTIVES

The primary objective of the ONR-307 instrument complement is to obtain the necessary data to construct models of the energetic particle and plasma environment of the Earth's radiation belts. The Medium Energy Ion Mass Spectrometer (IMS-HI) measures both the energetic ion composition energy spectra and pitch angle distributions, and the energetic neutral particle energy spectra and pitch angle distributions, with good mass, temporal, spatial, and energy resolution. The IMS-HI is located at an angle of  $75^\circ$  to the spin axis to maximize pitch angle sampling. The ion energy range is approximately 20 to 8000 keV-AMU/ $q^2$ .

The IMS-HI extends the energy range of ion composition measurements well above that of the traditional IMS-LO instruments, which are also part of the ONR-307 Experiment. The principle of the IMS-HI is based on ion momentum separation in a magnetic field followed by energy and mass defect analysis using an array of cooled silicon solid state sensors. The technique of cooling solid state

detectors for high resolution ( $< 2$  keV FWHM) energetic ion measurements in spacecraft instruments was reviewed by Voss et al<sup>1</sup> and was successfully demonstrated in the Stimulated Emission of Energetic Particles (SEEP) experiment on the S31-1 satellite.<sup>2</sup> The IMS-HI features a parallel architecture with simultaneous mass and energy analysis at relatively high sensitivity.

## 2. APPLICATIONS

One of the key unknowns of the radiation belt models is the medium energy ( $30 < E < 600$  keV) ion composition of the Earth's ring current.<sup>3</sup> The reason is that the major part of the ring current plasma falls in the gap between measurements of ion composition by traditional electrostatic and magnetic deflection systems ( $E < \sim 30$  keV) and measurements by differential energy loss and total energy deposition in solid state detector instruments ( $E > \sim 600$  keV). The IMS-HI incorporates elements of these two traditional techniques to measure directly this important energy/mass range that is not accessible by application of either traditional technique independently.

A knowledge of the ring current ion composition is important from a geophysical standpoint and for obtaining an accurate radiation belt model to correctly predict electronic component and material irradiation effects. It is known, for example, that the irradiation effects on materials such as thermal control surfaces on long-lived satellites is strongly dependent on the mass of the impinging ions. This is particularly important at geosynchronous altitudes.

Lyons and Evans,<sup>4</sup> Spjeldvik and Fritz,<sup>5</sup> and Tinsley<sup>6</sup> have demonstrated the

1. Voss, H.D., Reagan, J.B., Imhof, W.L., Murray, D.O., Simpson, D.A., Cauffman, D.P., and Bakke, J.C. (1982) Low temperature characteristics of solid state detectors for energetic x-ray, ion and electron spectrometers, IEEE Trans. Nucl. Sci. 29:164.
2. Imhof, W.L., Reagan, J.B., Voss, H.D., Gaines, E.E., Datlowe, D.W., Mobilia, J., Helliwell, R.A., Inan, U.S., Katsufakis, J., and Joiner, R.G. (1983) The modulated precipitation of radiation belt electrons by controlled signals from VLF transmitters, Geophys. Res. Lett. 10:8, 615.
3. Williams, D.J. (1979) Ring current composition and sources, in Dynamics of the Magnetosphere, S.I. Akasofu, Ed., D. Reidel, Dordrecht, Holland, pp. 407-424.
4. Lyons, L.R., and Evans, D.S. (1976) The inconsistency between proton charge exchange and the observed ring current decay, J. Geophys. Res. 81:6197.
5. Spjeldvik, W.N., and Fritz, T.A. (1978) Energetic ionized helium in the quiet time radiation belts: Theory and comparison with observations, J. Geophys. Res. 83:654.
6. Tinsley, B.A. (1978) Effects of charge exchange involving H and H<sup>+</sup> in the upper atmosphere, Planet. Space Sci. 26:847.

importance of including ions and neutrals other than protons to explain the decay rates observed in the ring current recovery phase. The ions of the ring current, by charge exchange with thermal hydrogen atoms, become neutrals and can thus escape from the Earth's environment. This is a significant loss process of the ring current medium energy ions.<sup>6</sup> A relatively small percentage of these ions are directed toward the Earth, where they ionize the low latitude atmosphere. These can be used as tracers of the ring current composition.

Low altitude satellite measurements of energetic ions associated with the ring current have been reported by Moritz<sup>7</sup> and Mizera and Blake;<sup>8</sup> helium emissions have been measured by Meier and Weller.<sup>9</sup> Rocket measurements of helium and hydrogen at the equator during the ring current recovery phase were reported by Voss and Smith.<sup>10</sup> Measuring the ring current energetic neutrals over the regions of space covered by the CRRES orbit will provide additional information on the ring current decay rates, spatial geometry, and temporal changes weighted by the appropriate cross sections and neutral hydrogen density. Both the direct medium energy ion composition and the indirect neutral atom tracers can be analyzed with the IMS-HI Spectrometer.

### 3. MEASURING TECHNIQUES

The IMS-HI is based on ion momentum separation in a magnetic field followed by energy and mass defect analysis using an array of cooled silicon solid state sensors as shown in Figure 49. The entrance collimator defines the ion beam angular resolution using a series of rectangular baffles and includes a broom magnet to reject electrons with energy less than 1 MeV.

At the collimator exit, an annular solid state detector with a central hole measures the integral ion and neutral energy spectrum of the beam supplied to the magnet for momentum analysis. A 7-kG magnetic field then disperses the collimated ions onto a set of six passively cooled (-50°C) silicon surface barrier detectors. The energy range, which varies with ion species, is approximately

7. Moritz, J. (1972) Energetic protons at low equatorial altitudes: A newly discovered radiation belt phenomenon and its explanation, J. Geophys. Res. 38:701.
8. Mizera, P.F., and Blake, J.B. (1973) Observations of ring current protons at low altitudes, J. Geophys. Res. 28:1058.
9. Meier, R.R., and Weller, C.S. (1975) Observations of equatorial EUV bands: Evidence for low-altitude precipitation of ring current helium, J. Geophys. Res. 80:2813.
10. Voss, H.D., and Smith, L.G. (1980) Rocket observations of energetic ions in the nighttime equatorial precipitation zone, Space Res. 20:149.

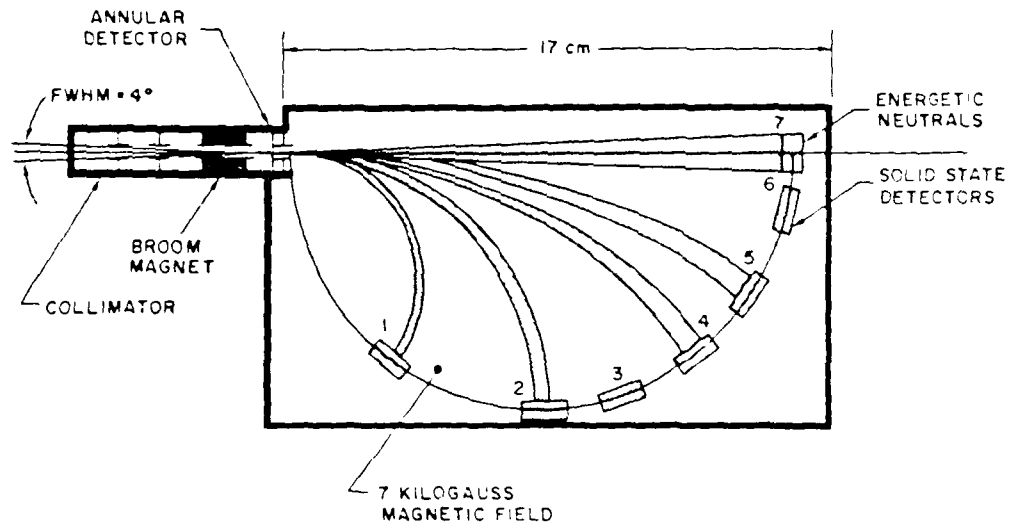


Figure 49. Schematic Diagram of the Medium Energy Ion Mass Spectrometer (IMS-HI)

$EM/q^2 = 20-8000 \text{ keV-AMU}/q^2$ . A seventh sensor, located directly in line with the collimator, measures energetic neutrals (ion rejection is approximately  $100 \text{ MeV-AMU}/q$ ).

The instrument features simultaneous mass and energy analysis at relatively large geometrical factors ( $10^{-3}$  to  $10^{-2} \text{ cm}^{-2} \text{ ster}$ ). Simultaneous measurements of charge states can be identified for each  $M/q^2$  and for the same  $M/q^2$ , in some cases, within the solid state detector due to dead zone and mass defect energy losses for equal  $M/q^2$  (for example,  $O^{++}$  and  $He^+$ ). Because of the multisensor design and parallel processing electronics, the dynamic range in flux covered is approximately six orders of magnitude.

A simulation of the ion separation in a 7-kG magnetic field is shown in the position-energy diagram of Figure 50. The image plane, S, is defined as the arc length, beginning at the collimator, for a radius,  $R=9 \text{ cm}$ . Solid-state detectors 1-7 are located at angle,  $\theta$ , of  $40^\circ$ ,  $65^\circ$ ,  $90^\circ$ ,  $115^\circ$ ,  $140^\circ$ ,  $165^\circ$ , and  $179^\circ$ , respectively. Solid state detectors 1-6 are n-type silicon having either 20 or 40 grams  $\text{cm}^{-2}$  of gold surface deposit. The neutral and annular detectors are of p-type silicon to improve light rejection and radiation damage sensitivity. The mass defect in solid state detectors results from energy loss of non-ionizing nuclear collisions within the solid that reduce the efficiency of electronic signal generation. The mass defect increases with atomic weight of the nuclei in a well un-

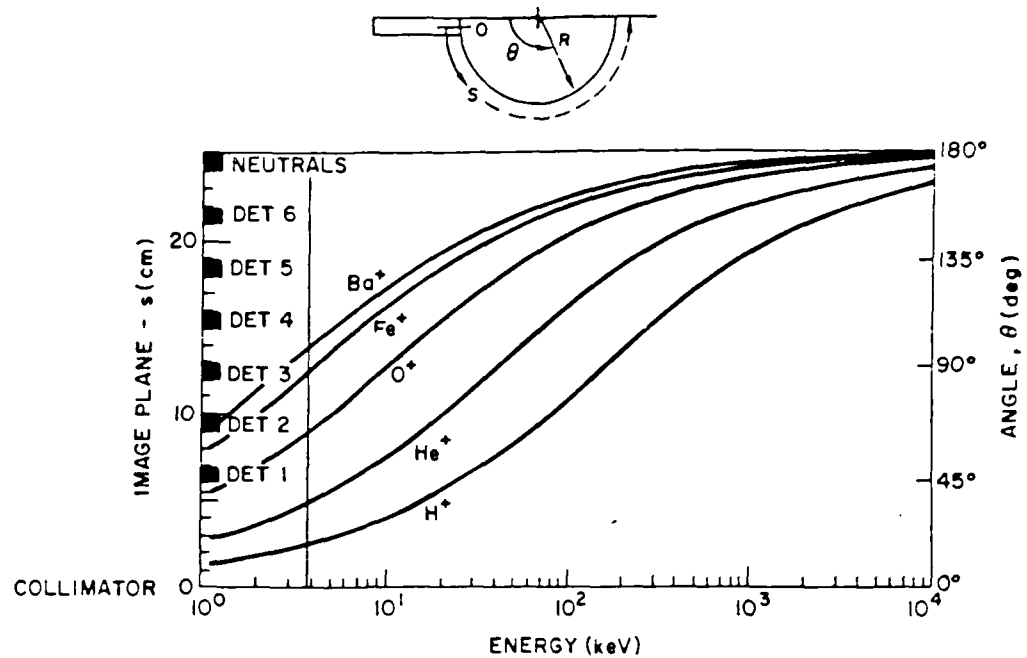


Figure 50. Position-Energy Plot for the Medium Energy Ion Mass Spectrometer (IMS-HI) for Singly Charged Ions in a 7-kG Magnetic Field

derstood way,<sup>11</sup> and causes further mass separation, with commensurate energy scatter, for the heavier nuclei.

The magnet section consists of a yoke, pole pieces, and a rare earth permanent magnet. To produce a homogeneous magnetic field of about 7000 G in the 5-mm gap and minimize weight, the best commercially available magnetic material (SmCo<sub>5</sub> with 25 MGOe energy product) is used. The yoke completely surrounds the magnetic field, permitting one to reduce the magnetic resistivity in the return flux section and to minimize the magnetic stray fields. Shape and dimensions are optimized to save weight and to assure a uniform magnetic induction anywhere within the yoke. The resultant complex shape necessitates the use of numerical machining methods to meet the weight requirement and design goal of  $< \sim 100$  nT magnetic stray field at a distance of 1 meter. A yoke material (Hyperco 50) that possesses relatively high permeability (2000-4000) at high induction levels (20 kG) was chosen. The design weight of the 7-kG flight magnet assembly is about 5.7 kilograms.

11. Fercinal, G., Siffert, P., and Coche, A. (1968) Pulse height defects due to nuclear collisions measured with thin window silicon surface barrier detector, *IEEE Trans. Nucl. Sci.* (NS-15):475.

#### 4. FUNCTION BLOCK DIAGRAM

A function block diagram of the IMS-HI is shown in Figure 51. Variable pulse height signals from the ion sensors are each routed for analysis to a peak detector circuit and analog multiplexer. Each peak detector circuit is allowed to track and hold the highest peak value for input pulses below the programmable threshold,  $V_T$ , and to hold and stop sampling for input pulses above  $V_T$ . The sample interval for each detector is 45  $\mu$ sec. The read and reset of each peak detector circuit is controlled by the master clock strobes so that a continuous and sequential scan is made of each detector.

Simultaneous with the reset command, the 256-channel analog-to-digital converter is activated, and the resulting digital pulse height (8 bits) is placed on the address bus of the energy look-up table. Also placed on the address bus of the RAM are the 3 bits that specify which detector is being processed. The content of this memory cell (16 bits) is read into the accumulator, incremented by one, and then read back into the memory cell. An address counter is then used to sequentially step through the entire RAM for telemetry readout. A data compressor packs the 16-bit sum into an 8-bit byte for serial interface with the satellite telemetry.

The two basic modes of instrument operation are Mass Lock and Mass Scan. In the Mass Scan mode, each of the seven solid state sensors is pulse height analyzed into 256 levels of which 64 intervals are accumulated in memory and read out every eight seconds. This mode is used to scan all mass peaks within the range of the sensor relative to the background continuum. In the Mass Lock mode, each of the seven solid state sensors is pulse height analyzed into 256 levels, of which four intervals (typically, four ions) are accumulated in memory and read out every half second. This mode is used for making rapid spectral snapshots of four ions as a function of pitch angle. Baseline operation of the instrument will be a toggle mode (32.768 sec) between the Mass Lock mode and the Mass Scan mode.

#### Acknowledgments

The authors wish to thank T.C. Sanders, D.A. Simpson, L.A. Hooker, and V.F. Waltz for their efforts in the design, development, and fabrication of this instrument. We also deeply appreciate the assistance of R.D. Sharp and Jack Quinn.

This effort was supported by the Office of Naval Research under contract N00014-83-C-0476 and by the Lockheed Independent Research Program.

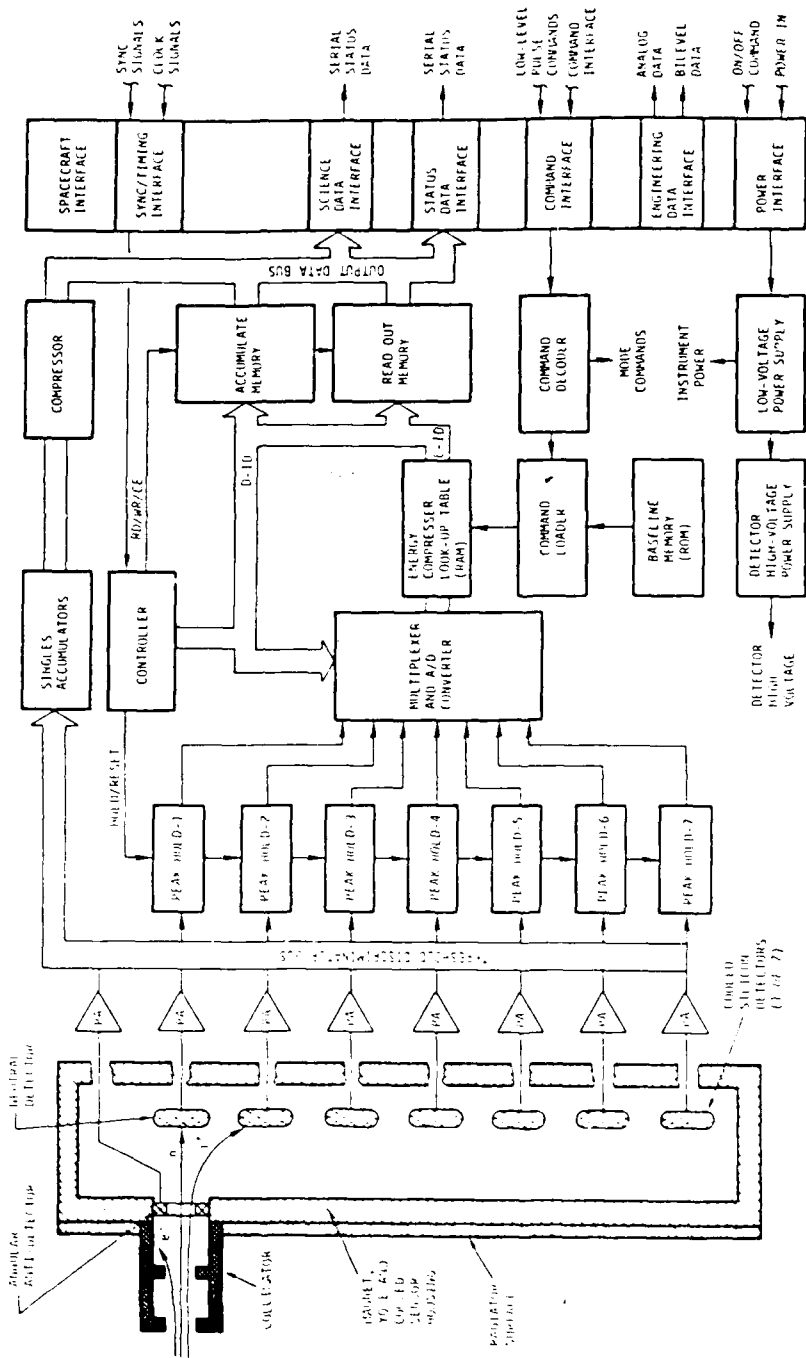


Figure 5.1. Function Block Diagram for the Medium Energy Ion Mass Spectrometer (IMS-III)

## References

1. Voss, H.D., Reagan, J.B., Imhof, W.L., Murray, D.O., Simpson, D.A., Cauffman, D.P., and Bakke, J.C. (1982) Low temperature characteristics of solid state detectors for energetic x-ray, ion and electron spectrometers, IEEE Trans. Nucl. Sci. (NS-29):164.
2. Imhof, W.L., Reagan, J.B., Voss, H.D., Gaines, E.E., Datlowe, D.W., Mobilia, J., Helliwell, R.A., Inan, U.S., Katsufakis, J., and Joiner, R.G. (1983) The modulated precipitation of radiation belt electrons by controlled signals from VLF transmitters, Geophys. Res. Lett. 10:3, 615.
3. Williams, D.J. (1979) Ring current composition and sources, in Dynamics of the Magnetosphere, S.I. Akasofu, Ed., R. Reidel, Dordrecht, Holland, pp. 407-424.
4. Lyons, L.R., and Evans, D.S. (1976) The inconsistency between proton charge exchange and the observed ring current decay, J. Geophys. Res. 81:6197.
5. Spjeldvik, W.N., and Fritz, T.A. (1978) Energetic ionized helium in the quiet time radiation belts: Theory and comparison with observations, J. Geophys. Res. 83:654.
6. Tinsley, B.A. (1978) Effects of charge exchange involving H and H<sup>+</sup> in the upper atmosphere, Planet. Space Sci. 26:847.
7. Mortiz, J. (1972) Energetic protons at low equatorial altitudes: A newly discovered radiation belt phenomenon and its explanation, J. Geophys. Res. 38:701.
8. Mizera, P.F., and Blake, J.B. (1973) Observations of ring current protons at low altitudes, J. Geophys. Res. 28:1058.
9. Meier, R.R., and Weller, C.S. (1975) Observations of equatorial EUV bands: Evidence for low-altitude precipitation of ring current helium, J. Geophys. Res. 80:2813.
10. Voss, H.D., and Smith, L.G. (1980) Rocket observations of energetic ions in the nighttime equatorial precipitation zone, Space Res. 20:149.

11. Forcinal, G., Siffert, P., and Coche, A. (1968) Pulse height defects due to nuclear collisions measured with thin window silicon surface barrier detector, IEEE Trans. Nucl. Sci. (NS-15):475.

APPENDIX D

STATEMENT OF CONFORMANCE  
FOR ONR-307 PAYLOAD

Contract: N00014-83-C-0476

BASD/CRRES ICD: CRRES-227  
CRRES-228

This certifies that the following listed contract end items have been fabricated, inspected, calibrated, tested and documented, as indicated herein, in accordance with applicable contractual documents. Results of prescribed tests and inspections indicate conformance to all contract requirements, except as otherwise indicated.

DELIVERABLES

Item 1 - ONR-307 Flight Hardware:

- a. ONR-307-3-1 SEP Sensor Package
- b. ONR-307-3-2 SEP Analyzer Package
- c. ONR-307-8-1 IMS-L01
- d. ONR-307-8-2 IMS-L02
- e. ONR-307-8-3 IMS-HI
- f. SEP-IH Interconnect Harness (PN11860-101;SN-01)
- g. 3 ea. Arc Suppression Assembly (PN12785-101;SN-02,03,04)

Item 2 - Acceptance Data Package consisting of the following items:

- a. ICD Compliance Summary (LMSC/F067868A).
- b. Acceptance Test Plan (Redlined) (LMSC/F067866).
- c. Electromagnetic Compatibility Test Data Package (LMSC/F067882).
- d. Thermal-Vacuum Test Data Package (LMSC/F067877).
- e. Random Vibration Test Data Package (LMSC/F067878).
- f. Mass Properties Data Package (LMSC/F067879).
- g. Stress/Fracture Analysis (LMSC/F018849).
- h. Safety/Hazard Analysis (LMSC/F067881).
- i. Flight Configuration Power Estimates
- j. Redlined Mechanical Drawings Showing "As-Built" Configuration

Instrument Package

Drawing Number/Rev

|             |         |
|-------------|---------|
| ONR-307-3-1 | 11503/F |
| ONR-307-3-2 | 11404/G |
| ONR-307-8-1 | 11405/F |
| ONR-307-8-2 | 11405/F |
| ONR-307-8-3 | 11759/F |

k. Mechanical Configuration Drawings Identifying Part Number and Locations of Redtag and Greentag items

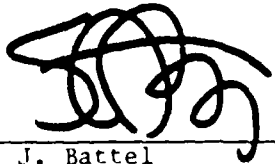
| <u>Instrument Package</u> | <u>Drawing Number/Rev</u> |
|---------------------------|---------------------------|
| ONR-307-3-1               | 11780/A                   |
| ONR-307-3-2               | 11768/A                   |
| ONR-307-8-1               | 11778/A                   |
| ONR-307-8-2               | 11778/A                   |
| ONR-307-8-3               | 11760/D                   |

A compliance summary, which identifies waivers and deviations is attached as Appendix-A of this document.

The following requested data are not included as part of this Acceptance Data Package for the reasons specified:

- a. Acoustic - Testing to be performed at spacecraft level only.
- b. Functional/Calibration - Data other than those required for formal acceptance test testing are contained in logbooks which are proprietary to LMSC. All test data are available to government representatives for on-site inspection. Monitor calibration data is in preparation and will be submitted at the time of instrument delivery.
- c. Shock - Testing to be performed at the spacecraft level only.
- d. Magnetic Field Report - Testing to be performed by BASD.
- e. Radioactive Scan Report - Flight detectors for the ONR-307-3-1 package which contain radioactive sources, are not installed for initial delivery. Therefore, a radioactive scan was not performed.
- f. Special Handling Requirements Update - No special handling requirements are required besides those specified in the ICD or previously provided.
- g. GSE Documentation - No GSE equipment will be interfaced to the ONR-307 Payload when it is on the CRRES Satellite.

Certified By: \_\_\_\_\_

  
 S. J. Battel  
 ONR-307 Program Manager

7/15/86

COMPLIANCE SUMMARY

The following general requirement areas have been reviewed and are certified as being compliant unless otherwise noted. Any noted non-compliances, along with either the reason(s) for non-compliance or the corrective action(s) that were/will be taken, are described on the following pages. For a detailed review of ICD compliance see the ONR-307 ICD Compliance Summary (LMSC/F067868A) which has been provided as part of the Acceptance Data Package.

| <u>REQUIREMENT</u>                    | <u>COMPLIANT (Yes/No)</u> |
|---------------------------------------|---------------------------|
| 1. Safety and reliability             | Y                         |
| 2. Physical interfaces                |                           |
| a. Mechanical                         | N (Note 1)                |
| b. Electrical                         | N (Note 2)                |
| c. Mechanical GSE                     | Y                         |
| d. Electrical GSE                     | Y                         |
| 3. Environmental interfaces           |                           |
| a. Structural                         | Y                         |
| b. Thermal                            | Y (Note 3)                |
| c. Mass properties                    | Y                         |
| d. Magnetic fields                    | Y (Note 4)                |
| e. Temperature                        | N (Note 5)                |
| f. Humidity                           | Y                         |
| g. Cleanliness                        | Y                         |
| h. Dynamic (shock/vibration/acoustic) | N (Note 6)                |
| 4. Functional interfaces              |                           |
| a. Power                              | Y (Note 7)                |
| b. EMC                                | Y (Note 8)                |
| c. Commanding                         | Y                         |
| d. Telemetry                          | Y                         |
| e. Isolation                          | N (Note 9)                |

## NOTES ON COMPLIANCE

1. Supplied "As-Built" mechanical configuration drawings accurately represent existing instrument design. The existing configuration differs slightly from ICD drawings. BASD is aware of these variances and has prepared a PIRN which documents them.

A test non-conformance (See NCR-1 included in ONR-307 Random Vibration Test Report-LMSC/F067878) has been identified for the ONR-307-8-3 instrument which will require a design modification. The plan for this modification has been documented in a letter to STP (S. Battel to Maj. Trever, 3 July 1986) which is included herein as Appendix-B.

2. Some minor variances to the electrical interface exist with BASD cognizance. These items are identified and discussed in the ONR-307 ICD Compliance Summary -LMSC/F067868. BASD has prepared a PIRN for all items.
3. A final thermal model update for the ONR-307-8-3 instrument is in process. This update is being performed with BASD cognizance and will be provided before instrument delivery.
4. Magnetic field measurements will be performed by BASD. It is estimated that the ONR-307-3 and ONR-307-8-3 will have a residual magnetic field of < 100 $\gamma$  and 100 $\gamma$  to 180 $\gamma$  respectively. These estimates have been previously reported to STP.
5. The ONR-307-8-3 instrument sensor assembly has a cold survival and acceptable temperature limit of -90 $^{\circ}$ C and -70 $^{\circ}$ C respectively. Due to laboratory equipment limitations, it has not been possible to cycle the sensor temperature below -80 $^{\circ}$ C. Therefore -80 $^{\circ}$ C should be considered the new cold survival temperature limit. To exceed this lower temperature limit will change the sensor magnetic field strength and result in a change in instrument calibration.
6. As discussed in Note 1, a test non-conformance occurred on the ONR-307-8- instrument which will require a design modification before random vibration qualification can be completed. Shock and acoustic testing is to be performed at the spacecraft level only.
7. The ONR-307 instruments use substantially less power than their present allocation. This is the result of a commitment made by the ONR-307 program to reduce power and, in doing so, eliminate the need for duty cycling during extended shadow periods on-orbit. The expected flight power numbers are provided in the acceptance data package and have been provided to BASD as a PIRN.

8. The ONR-307-3 instrument is composed of two packages one of which, the ONR-307-3-1, is isolated from the Spacecraft in the flight configuration. During electrostatic discharge (ESD) testing in this configuration it was noted direct discharges to the ONR-307-3-1 package of potential greater than a few kilovolts (kv) induced instrument upsets. These upsets did not prove harmful but would require the execution of ground commands before useful data taking could resume if such upsets occurred on-orbit.

At voltages above 8 kv a latchup condition was noted on 1 of approximately 20 occasions of when an arc was drawn to the instrument enclosure. This latchup condition could not be reproduced on further testing and, therefore, could not be investigated in detail. It did not, however, appear to not be serious in that the power rise was not great and the instrument returned to a normal operating condition following a power ON/OFF cycle.

Following these observations, a telephone discussion was held with H. Koon concerning ESD test thresholds and instrument safety. He indicated that he had recommended only a radiated ESD test be performed on CRRES instruments and felt that a direct discharge was a useful sensitivity test but probably not necessary. Therefore, it was agreed that the test requirements would be modified such that instead of a 10 kv discharge, a discharge of increasingly high level (up to a maximum of 10 kv) would be applied to measure instrument ESD sensitivity. The maximum direct voltage applied would be limited to that which resulted in "safe" upsets and would not damage the instrument. The radiated ESD setting would remain 10 kv for all tests. The remaining instruments, when tested, proved not susceptible to either radiated or direct ESD.

9. Measurements between instrument chassis, signal return and power return consistently show capacitance readings of approximately  $0.13\mu\text{f}$  for each case. This value exceeds the  $0.1\mu\text{f}$  value specified in the ICD. A waiver is requested to allow this slightly large value. The alternative would be to disassemble the instruments and replace the present  $.1\mu\text{f}$  capacitors with lower values.

APPENDIX E

## ONR 307-3 CALIBRATIONS

The SEP sensor heads of the ONR 307-3 experiment were calibrated using electron and proton beams from accelerators at Goddard Space Flight Center and Harvard University in the time period from 7 April to 19 April, 1986.

Two accelerators were used at GSFC, a low energy electron machine with maximum energy of 150 keV and a Van de Graaf accelerator with maximum energies for electrons and protons of 1.5 MeV. For all of these runs, the sensors were in vacuum. All runs were at nominal room temperatures between about 18°C and 25°C.

High energy proton calibrations were done at the Harvard Cyclotron Laboratory. The cyclotron beam energy of 159 MeV is reduced by the use of absorbers yielding a beam energy spread of less than 5 MeV at energies greater than about 90 MeV. Below 90 MeV, this energy spread increases to about 15 MeV at 35 MeV. The sensors were in air for these runs.

The sensor heads include the flight detectors, preamplifiers and shaping amplifiers. The gains of these systems were measured with a Canberra Model 40 multichannel pulse height analyzer controlled by a microcomputer and other GSE as shown in Figure 1.

The initial runs at GSFC were energy calibrations with low energy electrons. Each sensor was exposed to nominal energies of 25, 30, 40, 60, 100 and 150 keV.

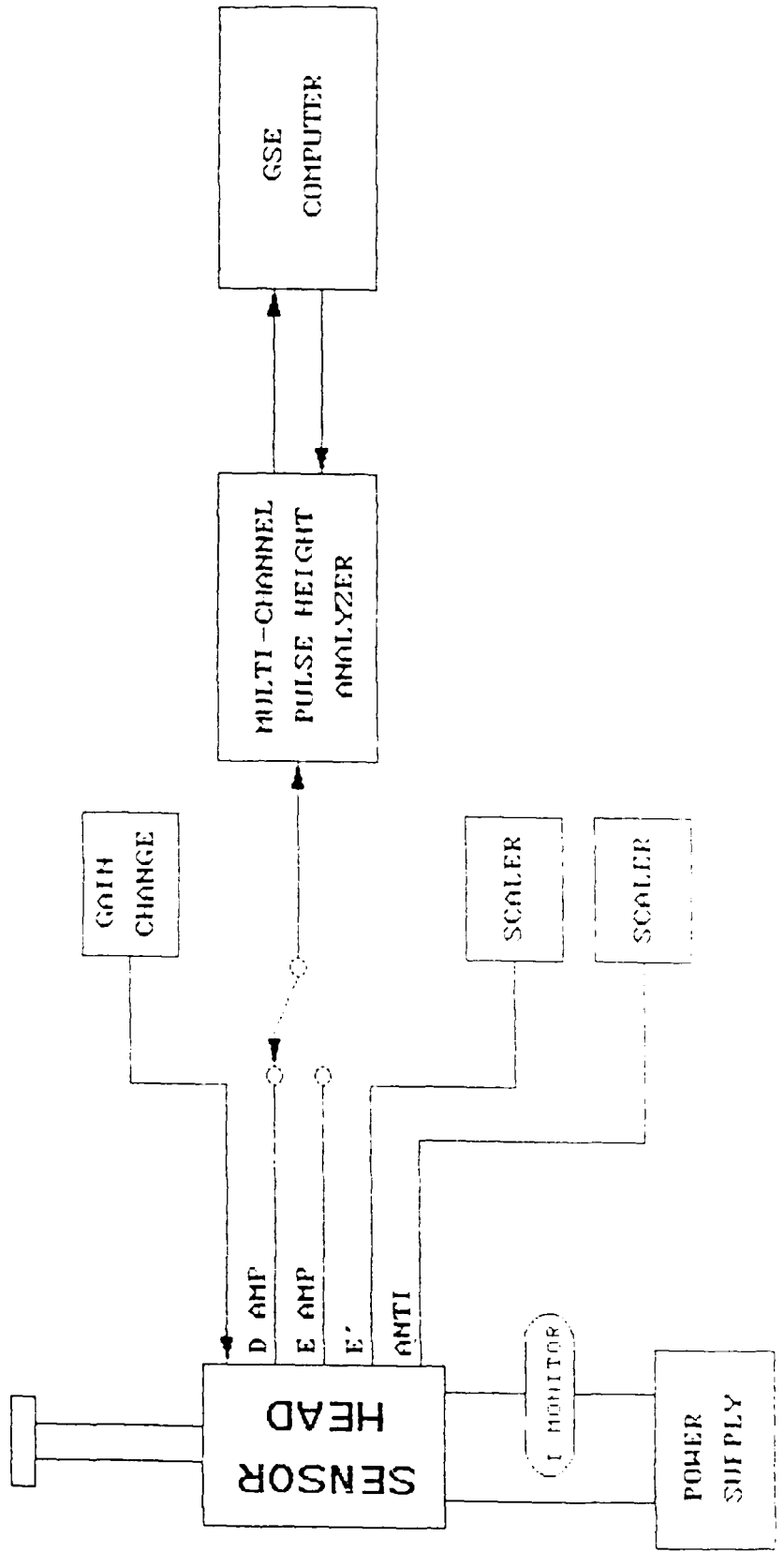
The beam rate from the low energy electron accelerator was kept between 1000 counts/s and 6000 counts/s, the variability being due to retuning the beam with a change in energy. For any given run, the beam rate was stable to about 25 percent. The results of these runs are shown in Figure 2.

The sensors were then individually installed in the Van de Graaf vacuum chamber. Head #1 was run first and was initially exposed to 147 keV electrons at a series of angular steps 0.2 to 0.3 degrees apart in order to determine the beam-collimator alignment and at the same time to measure the angular response

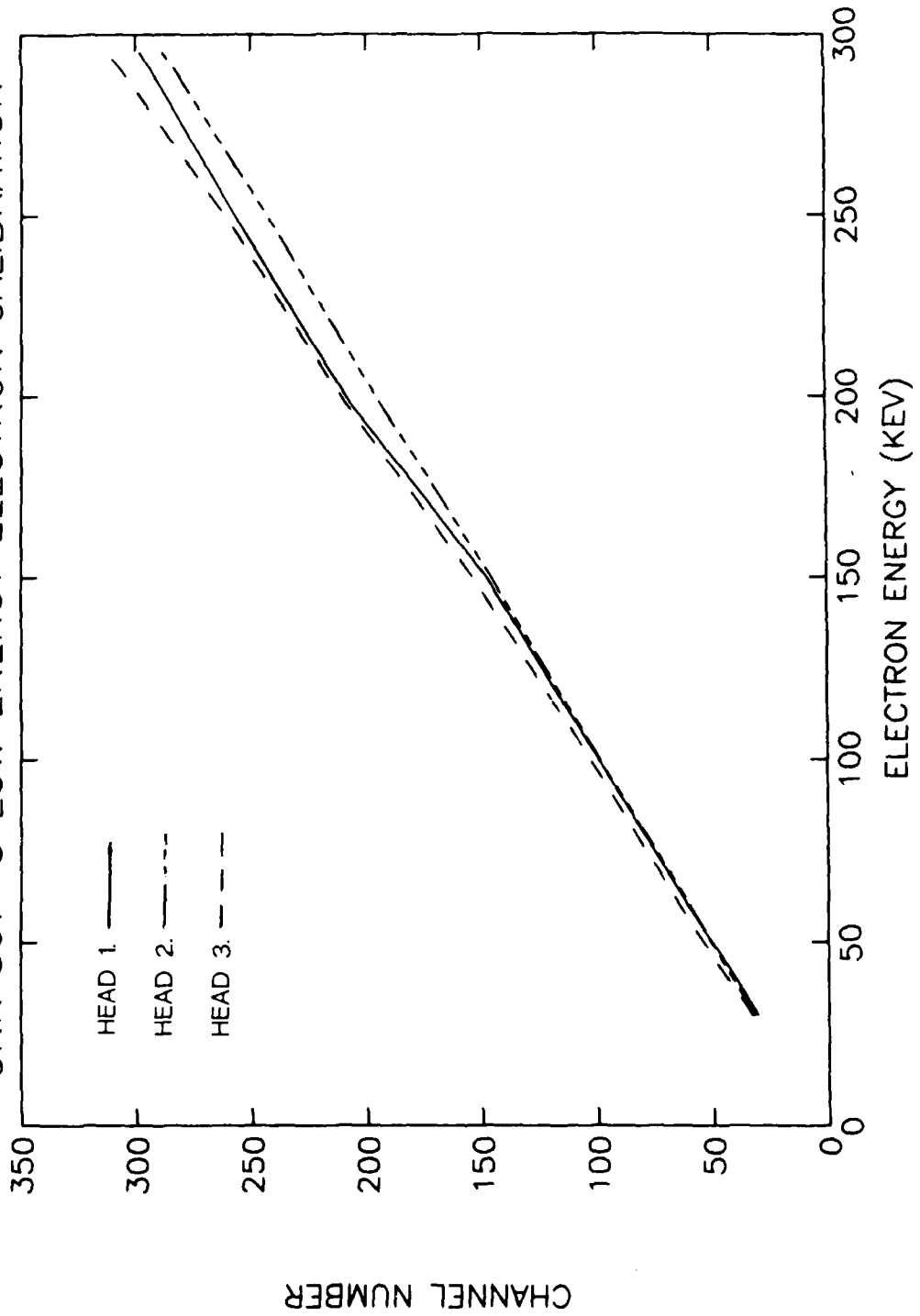
of the collimator. Figure 3. shows the angular definition of the Head #1 collimator to a collimated beam of low energy electrons. Then, at the center angle, electron energy calibrations were taken at 192, 248 and 295 keV in the DE/DX detector. High energy electron runs were made at 292, 384, 474, 970, and 1464 keV in the E detector. The electron beam flux from the Van de Graaf varied from 1200 counts/s to 2500 counts/s run to run. Head #2 was installed next and exposed to 150, 198, 248 and 297 keV electrons for the DE/DX calibration, and 296, 345, 394, 493, 1005 and 1487 keV electrons for the E detector. Head #3 was then calibrated with 150, 200, 248 and 300 keV electrons for the DE/DX detector and 299, 346, 395, 498, 1006 and 1490 keV electrons for the E detector. The Van de Graaf was then configured to accelerate protons and Head #3 was exposed to 494, 700, 1012, 1231 and 1500 keV protons. Head #2 was reinstalled and calibrated with 500, 698, 1008, 1204 and 1498 keV protons. Finally, Head #1 was calibrated with protons of 501, 700, 1004, 1210 and 1507 keV, completing the low energy particle runs at GSFC. The results of these calibrations are shown in Figures 4 and 5.

At the Harvard Cyclotron Laboratory, a precalibration run was made using a NaI scintillator furnished by the Laboratory to determine the energy spread of the beam at energies from 35 MeV to 148 MeV. The sensor heads were each exposed to the collimated proton beam at 35, 45, 55, 65, 75, 85, 95 and 100 MeV energies. During the sequence of runs, the E' detector singles rate was recorded at energies up to 90 MeV and the Anti rate recorded at 90 MeV and above. The high energy proton data presented in Figure 6. shows the expected peak in energy deposition at 45 MeV (the thickness of the DE/DX and E detectors is nominally 1.02 cm which is the range of 45 MeV protons in silicon). The measured energy deposition from higher energy protons penetrating the detectors is within 1 MeV of calculated values.

ONR 307-3 GSE CONFIGURATION



ONR 307-3 LOW ENERGY ELECTRON CALIBRATION



ONR 307-3 ANGULAR RESPONSE TO 150 KEV ELECTRONS

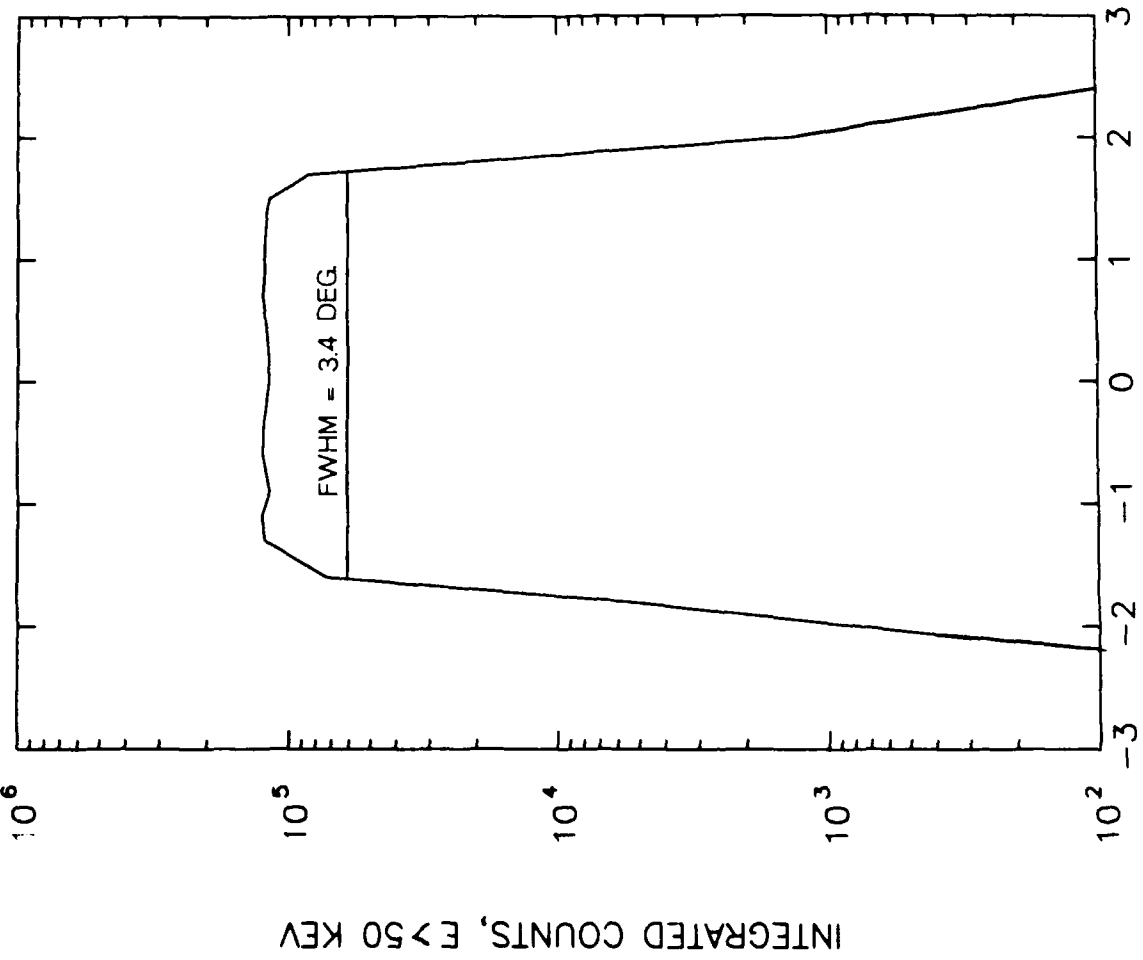
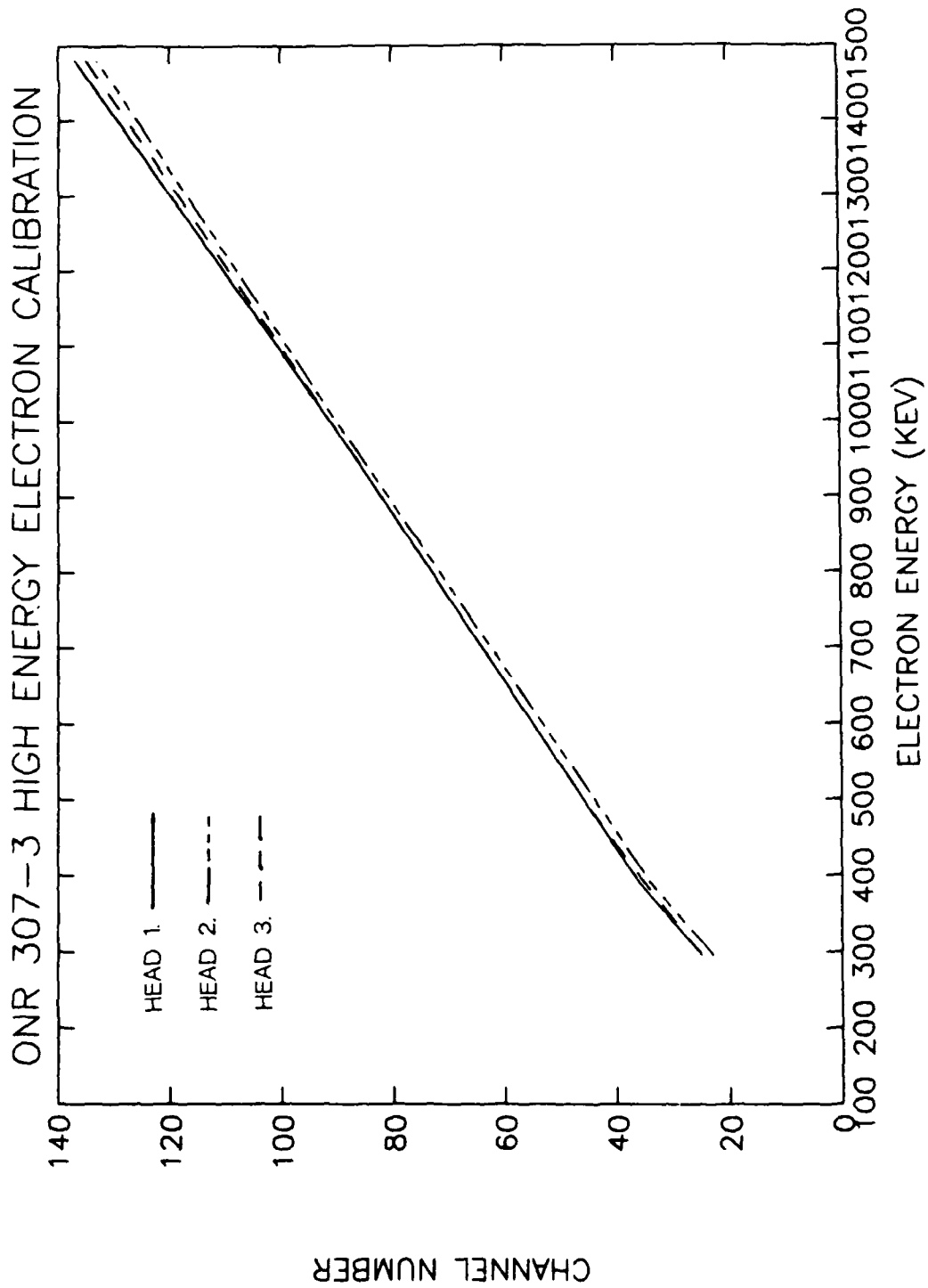


Figure 3.



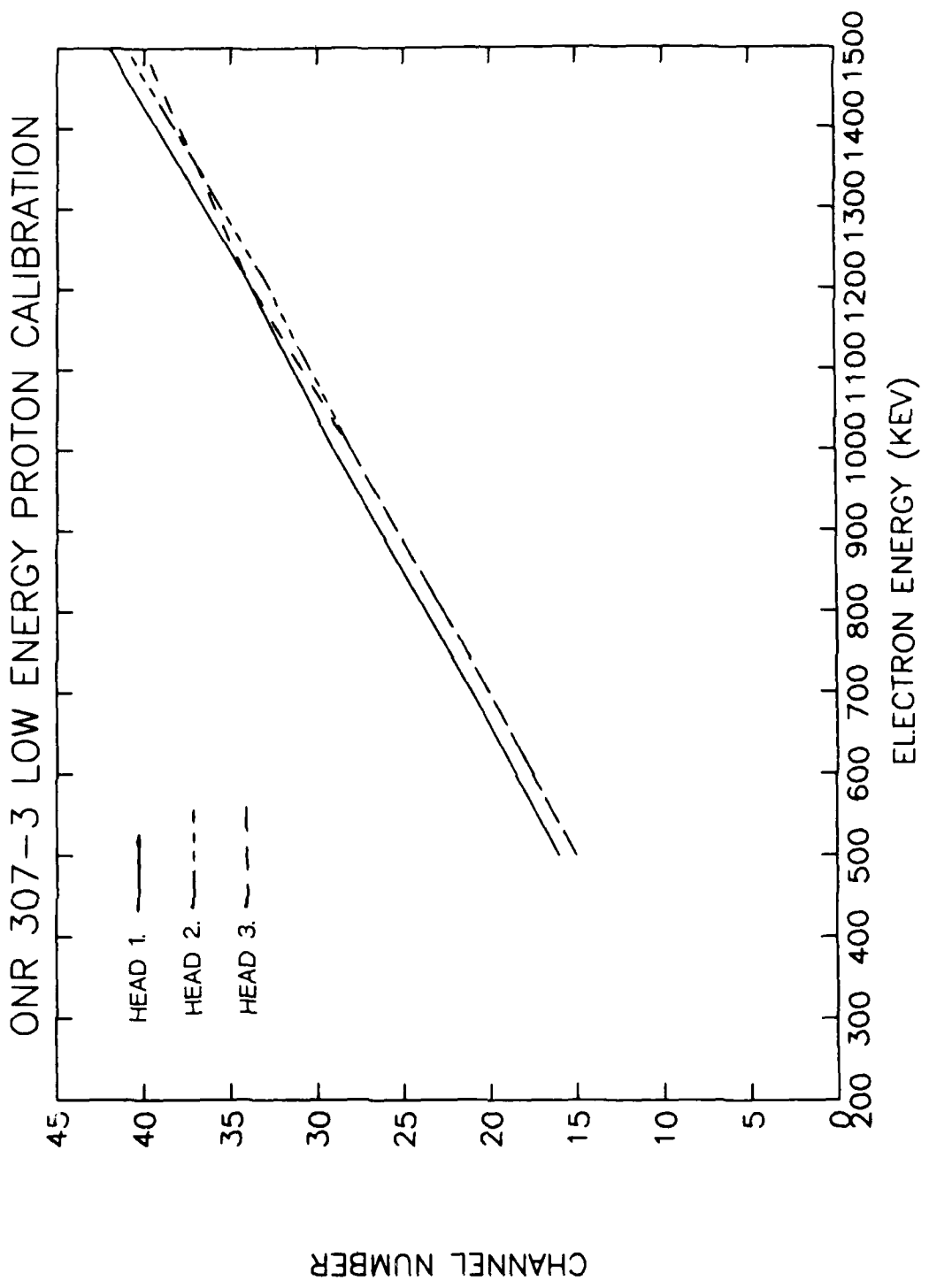


Figure 5.

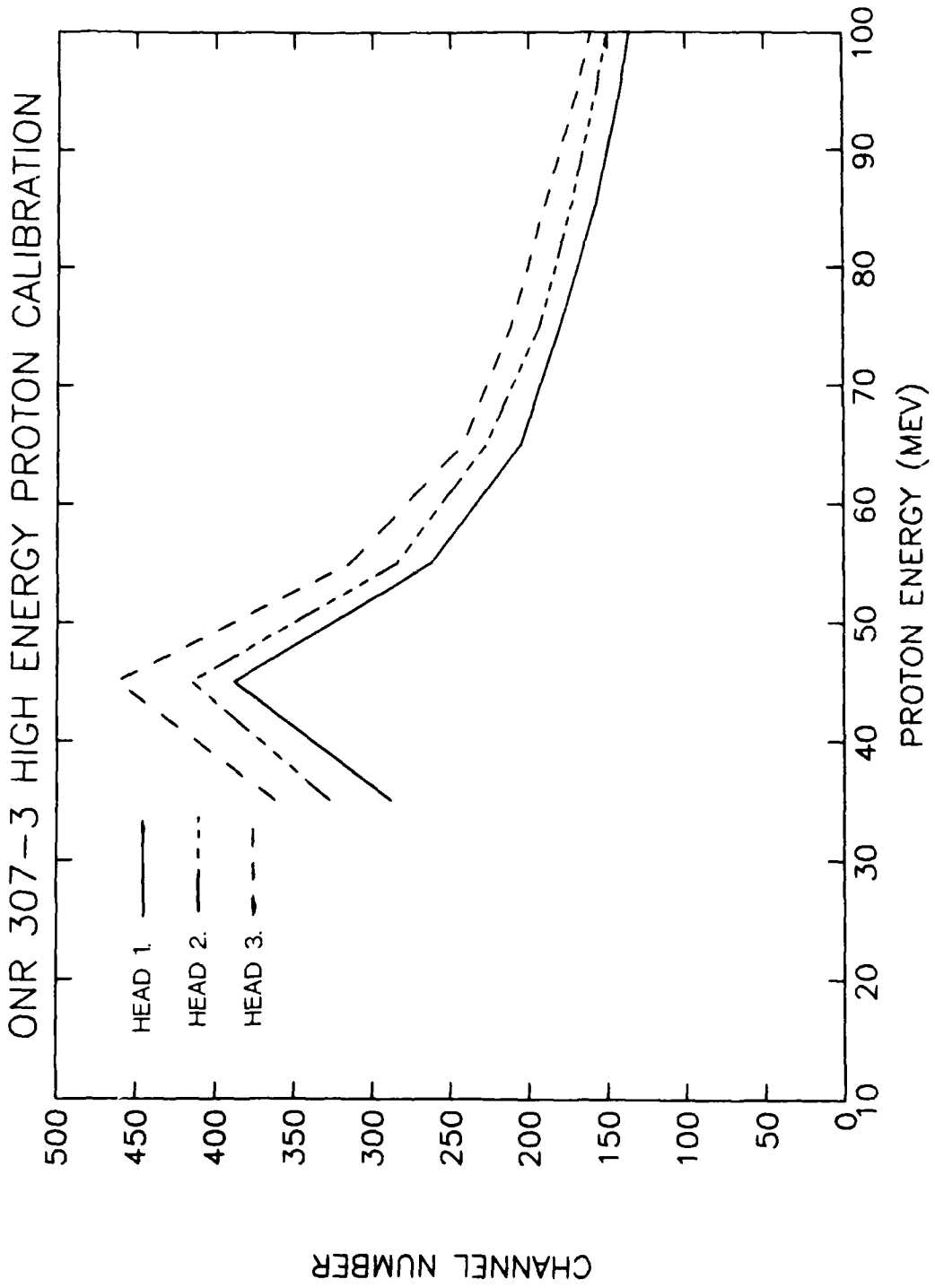


Figure 6.

DISTRIBUTION

Dr. Ralph Alewine  
Defense Advanced Research Projects  
Agency  
Arlington, VA 22209

Dr. Roger Anderson  
Department of Physics and  
Astronomy  
University of Iowa  
Iowa City, Iowa 52242

Dr. J.B. Blake  
M2/259  
Aerospace Corporation  
2350 E. El Segundo Blvd.  
El Segundo, CA 90245

Defense Nuclear Agency (2)  
ATTN: RRAE  
Washington, D.C. 20305

Defense Technical Information  
Center (12)  
Bldg. 5, Cameron Station  
Alexandria, VA 22314

Dr. Charles Eastwood  
NASA Headquarters, Code ES  
400 Maryland Ave., S.W.  
Washington, D.C. 20546

Lt. Robert Ellis  
NSSA/54, Bldg. 130  
P.O. Box 92960  
Los Angeles, CA 90009

Dr. Theodore Fritz  
ESS-8, MS d-430  
Los Alamos National Laboratory  
Los Alamos, NM 87545

Dr. Herbert Gursky  
Space Science Division  
Naval Research Laboratory  
Washington, D.C. 20375

Dr. Susan Gussenhoven  
AFGL/PHP  
Hanscom AFB, MA 01731

Dr. David Hardy  
AFGL/PHP  
Hanscom AFB, MA 01731

Mr. R Gracen Joiner (5)  
Code 1114SP  
Office of Naval Research  
800 North Quincy St.  
Arlington, VA 22217

Dr. Harry Koons  
M2/260  
Aerospace Corporation  
2350 E. El Segundo Blvd.  
El Segundo, CA 90245

Col. George Lasche  
Defense Advanced Research Projects  
Agency  
Arlington, VA 22209

Dr. Chung-Son Lin  
Code 4752  
Naval Research Laboratory  
Washington, D.C. 20375

Dr. Forrest Mozer  
Space Sciences Laboratory  
University of California  
Berkeley, CA 94720

Mr. E.G. Mullen  
AFGL/PHP  
Hanscom AFB, MA 01731

Director, Naval Research  
Laboratory  
ATTN: Code 2627  
Washington, D.C. 20375

Mr. Murray Perkins  
University of Chicago  
Enrico Fermi Institute  
933 East 56th St.  
Chicago, IL 60637

Dr. David Reasoner  
NASA/MSFC Code ES-23  
Huntsville, AL 35812

DISTRIBUTION

Dr. James Ritter  
Code 6631  
Naval Research Laboratory  
Washington, D.C. 20375

Dr. Paul Robinson  
JPL, MS144218  
4800 Oak Grove Drive  
Pasadena, CA 91109

Dr. Paul Rodriguez  
Code 4752  
Naval Research Laboratory  
Washington, D.C. 20375

Dr. Rita Sagalyn  
AFGL/PH  
Hanscom AFB, MA 01731

Dr. John Simpson  
University of Chicago  
Enrico Fermi Institute  
933 East 56th St.  
Chicago, IL 60637

Dr. Howard Singer  
AFGL/PHG  
Hanscom AFB, MA 01731

Major S. Sneegas (3)  
Space Test Program, CLTPS  
P.O. Box 92960  
Los Angeles, CA 90009

Mr. John Stone  
NASA/MSFC/FA-21  
Marshall Space Flight Center, AL  
35812

Mr. William P. Sullivan  
AFGL/PHG  
Hanscom AFB, MA 01731

Ms. Rebecca A. Taylor  
Code 1512  
Office of Naval Research  
800 North Quincy St.  
Arlington, VA 22217

Dr. Terry Trumble  
AFWL/POOC-2  
WPAFB, OH 45433

Mr. Edmund Trzcinski  
AFGL/LID  
Hanscom AFB, MA 01731

Dr. A.L. Vampola  
M2/259  
Aerospace Corporation  
2350 E. El Segundo Blvd.  
El Segundo, CA 90245

END

DATE

FILMED

11 - 88

DTIC

L